Synthesis and Chelating Properties of a Chiral D-Galactose-Derived Ethylene Diamine Ligand

And

Preparation of Sugar-Derived 1,2,3-Triazoles on a Soluble Polymer Support

By

Brian Scott Freeze

Submitted in Partial Fulfillment

of the Requirements

for the Degree of

Master of Science

in the Chemistry Program

SCHOOL OF GRADUATE STUDIES

YOUNGSTOWN STATE UNIVERSITY

June, 1999

SYNTHESIS AND CHELATING PROPERTIES OF A CHIRAL D-GALACTOSE-DERIVED ETHYLENE DIAMINE LIGAND
AND
PREPARATION OF SUGAR-DERIVED 1,2,3-TRIAZOLES ON A SOLUBLE POLYMER SUPPORT

Brian Scott Freeze

I hereby release this dissertation to the public. I understand this dissertation will be housed at the Circulation Desk of the University library and will be available for public access. I also authorize the University or other individuals to make copies of this dissertation as needed for scholarly research.

Signature: Brian Scott Freeze 6/4/99
Brian Scott Freeze

Approvals:

Peter Norris 6/4/99
Dr. Peter Norris
Thesis Advisor

John Jackson 6/4/99
Dr. John A. Jackson
Committee Member

Jeffrey Smiley 6/4/99
Dr. Jeffrey A. Smiley
Committee Member

Peter J. Kasvinsky 6/4/99
Dr. Peter J. Kasvinsky
Dean of Graduate Studies

Thesis Abstract

This work concerns two distinct projects. The first describes the synthesis, characterization, and chelating properties of a chiral, D-galactose-derived ethylene diamine ligand. Binding of this ligand to platinum and palladium metals is subsequently demonstrated. The second project involves the use of the soluble-polymer supported (liquid-phase) method in the synthesis of reversed-nucleoside analogues. A comparison of the liquid-phase method with standard solution-phase synthetic techniques is also provided.

Acknowledgements

I would first like to acknowledge the Department of Chemistry at Youngstown State University, specifically Dr. Mincey and Dr. Mike, for giving me the opportunity to pursue a Master's degree. Second, I would like to thank Sue Viglione for always coming through with the chemicals and equipment needed to keep the work proceeding smoothly. Third, I would like to thank the Graduate School here at YSU for funding trips to conferences and conventions.

Thanks to Dr. John Jackson for making sure that we always had dry solvents available to work with, and for reviewing this thesis, a task for which Dr. Jeff Smiley also earns my thanks. I am also very appreciative of Dr. Tim Wagner for all the time he spent collecting X-ray data and calculating crystal structures.

On a personal note, I would like to thank my family for supporting me through seven years (and counting) of college, never once pressing me to finally make up my mind on what I wanted to do. I would also like to give a special thanks to Jennifer Lynn Nagle, who has put up with me for four years and has always stood by my side and allowed me to pursue my goals, even when it meant sacrifices for us. Recognition also goes to Lana, Danny, Rob, Shelly, Special Chris, and everyone else who put up with me for two years here in the Master's program.

Finally, I would like to thank Dr. Peter Norris for his guidance, both in the lab and in the classroom, as well as for the ideas that led to the projects described in this thesis. Dr. Norris also deserves my gratitude for putting up with my many questions, and especially for pushing me to do more than I thought I could. Without his help, none of this would have been possible.

Table Of Contents

List Of Figures

Introduction

In-depth study of the carbohydrates and their chemistry began in the late 19th century with chemist Emil Fischer.[1] In the absence of today's sophisticated separation techniques and analytical methods, Fischer characterized the structure of D-glucose (by far the most abundant sugar in Nature) and its stereoisomers, a feat which earned him the second Nobel Prize in chemistry in 1902. Fischer's efforts laid the groundwork to be followed up by Haworth and Hudson, whose work consolidated and expanded on the field of carbohydrate chemistry.[1] In the 1950s, Lemieux introduced nuclear magnetic resonance spectroscopy to the field, and went on to contribute greatly to the synthesis of sugars and their derivatives. Lemieux has also been instrumental in elucidating the complex roles of carbohydrates in biological systems, a connection that is all the more important today. Lemieux's efforts have helped to carry the study of carbohydrates beyond its beginnings as an under-appreciated offshoot of organic chemistry to a field with extraordinary significance in biology, chemistry, and in turn industry.

Carbohydrates have long been known to play key roles in biological systems. They serve as a prime source of energy for organisms *via* the glycolytic pathway. Photosynthesis, on the other hand, involves plant's utilization of carbon dioxide from the atmosphere, along with sunlight, to synthesize sugars and also to produce oxygen. The DNA and RNA polynucleotides that encode the instructions for life are known to be composed, in part, of the carbohydrates 2-deoxyribose and ribose, respectively. More recently, carbohydrates have been found to be substrates for key enzymes in secondary metabolism. This discovery allowed a new route to antibiotic and antiviral drug strategies *via* synthetic inhibitors of these enzymes. Carbohydrates have also recently

been implicated in the mediation of cell surface interactions, indicating consequences in the immune response.

Naturally occurring carbohydrates are chiral compounds made up of 3 or more carbons each of which is usually attached to an oxygen. D-Glucose, for example, is a six-carbon sugar that can be found in nature in one of three different interrelated forms, shown below (Figure 1). The six-membered ring form (**A**) is termed the pyranose form.

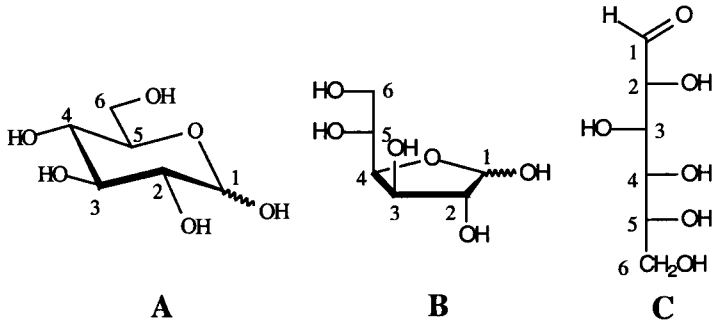

Figure 1. 3 Forms of D-Glucose

The five-membered ring furanose form is shown as **B**, and **C** is the straight-chain form, showing an aldehyde group at C-1. The orientation of the hydroxyl group at C-5 to the *right* in the straight-chain form defines the "D" configuration in the D-glucose nomenclature. Conversely, when the last stereocenter in the Fischer projection faces left, the sugar belongs to the L series. The orientation of the hydroxyl groups at the carbons numbered two through five determines this compound's identity as glucose. Changes in configuration, such as stereochemical inversion at the C-4 hydroxyl (to the left in the straight-chain form), results in a completely different sugar, in this case D-galactose. D-Galactose can also be found in cyclic forms, with the pyranose form having the hydroxyl at C-4 in the "up" direction, and the furanose form having the "flagpole" at C-4 in the "down" direction. Even the small change from glucose to galactose, for example, leads to a compound with completely different physical properties, spectroscopic properties,

biological properties, and reactivity, thus making carbohydrates very interesting (and often challenging) to work with. An interesting example of this concept is that while the human body can metabolize D-glucose for energy, its exact mirror image L-glucose can not be used by the body at all.

It should also be noted that the hydroxyl groups of the sugar are all in different chemical environments. There are primary, secondary, and, in the cyclic forms, uniquely reactive anomeric hydroxyl groups. In the cyclic forms the hydroxyl groups can be either axial or equatorial. Each of these variables contributes to the overall chemical versatility of carbohydrates, a feature that makes them very useful synthetically. It is this synthetic versatility, combined with the widespread applications mentioned previously, which prompts the ongoing interest in the field. The research to be described here will concentrate on two applications of carbohydrate-derived materials. The first project makes use of the inherent chirality of the carbohydrates to develop a novel chiral ligand to be complexed with metals. The second involves the synthesis of nucleoside analogs containing a furanose ring bound to a nitrogen-containing heterocycle.

The common thread between the two projects is found in the use of azido-deoxy sugar intermediates. Organic azides are a class of completely synthetic materials (no naturally occurring ones have ever been documented),[2] that contain the functional group shown below in its two major resonance forms (Figure 2). Study of azides began in the late 1800's with Curtius, who studied rearrangement chemistry of the azido group.[3] Since then, it has been found that in addition to undergoing rearrangements, azides can act as the dipole component in 1,3-dipolar cycloaddition reactions, and can be readily reduced to amines. The current research will combine this synthetic flexibility of the azide group

with the favorable properties (built-in chirality, variable solubility, ease of functionalization, etc.) of carbohydrates to synthesize potentially useful compounds.

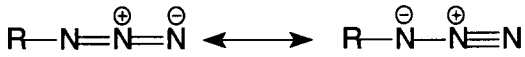

Figure 2. Resonance Forms Of The Azide Functionality

Project 1 - Introduction

Chirality is one of the most studied areas in synthetic organic chemistry. One key reason for this is the fact that almost every natural product found in biology is chiral. For example, all of the amino acids that make up the protein building blocks for life belong to the L-series. It is only these amino acids, and not their mirror image D-enantiomers, that can be used to build proteins. On the other hand, most carbohydrates found in nature belong to the D-series, and it is only these that can be metabolized for energy. Along the same lines, if chemists need to create a molecule that is active in an organism, they usually must pay close attention to the configuration of each stereocenter in the desired target. An example of the importance of this concept is the thalidomide tragedy of the 1960's. The (*R*)-enantiomer of the drug exhibits the desirable powerful analgesic properties. The (*S*)-enantiomer, on the other hand, shows no analgesic properties, and instead is a powerful teratogen.[4] It is because of issues like these that chirality, transference of chirality, and the synthesis of enantiomerically pure compounds are so important in synthesis today.

There are three major strategies for obtaining a single enantiomer of a given chiral compound. The first is by chromatographic resolution of a mixture of the two enantiomers. This method has a drawback in that the physical properties of the enantiomers are essentially the same are impossible to separate *via* conventional

chromotography. This drawback can be overcome *via* the use of an enantiomerically pure reagent or, more recently, *via* chiral column chromotography, but these methods also have drawbacks. A second method involves the use of naturally occurring chiral substrates as starting material. These can lead to enantiopure products fairly readily, but the possibilities for this method are potentially limited by the scope of known chiral compounds. A third method for procuring pure enantiomers is to convert a prochiral precursor into a chiral product. This is done by way of asymmetric synthesis. This method requires a chiral auxiliary that is used, ideally in catalytic amounts, to induce the substrates of a reaction to produce one enantiomer in excess over the other.[4]

Many compounds are known to induce asymmetry into a prochiral substrate. For example, Aldrich now sells a compound known as Jacobsen's catalyst (Figure 3), that is known to catalyze cyclopropanation or epoxidation reactions with high enantiomeric

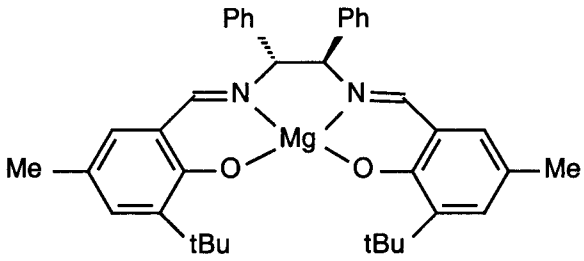

Figure 3. Jacobsen's Catalyst

excesses.[5] This compound has several disadvantages, however. It is not soluble in water; it is highly toxic; it is not very "environmentally friendly;" all of which are downfalls of such a system. If one could mimic the asymmetric induction of compounds like this with a carbohydrate analog, many of these drawbacks could be overcome.

The idea of using carbohydrates as chiral starting materials is not a new one. More recently, however, carbohydrates have found new uses as chiral auxiliaries.

Seyden-Penne's compilation "Chiral Auxiliaries and Ligands in Asymmetric Synthesis" highlights several references to 1,2:5,6-di-*O*-isopropylidene-D-glucopyranose (shown below, Figure 4), for applications such as selective protonation of a substrate bearing chiral residues, or asymmetric allylations. This latter use involves the carbohydrate as a ligand complexed with a titanium core, making use of the natural complexing capabilities of the sugar.

The current research will take a different approach to the formation of the sugar-derived catalytic complex, making use of the ethylene diamine moiety. Ethylene diamine compounds are known to be excellent agents for complexing with a wide variety of metals. Examples of this include cobalt, palladium, and platinum[6] complexes, among many others. The ethylene diamine functionality is also found in Jacobsen's catalyst (Figure 3), as well as in many derivatives of the powerful cancer-fighting agent cisplatin.[7]

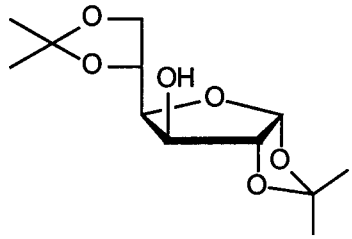

Figure 4. 1,2:5,6-di-*O*-isopropylidene-D-glucopyranose

The first project to be described here will bring together the topics and concepts mentioned above into the synthesis of a carbohydrate-derived ethylene diamine ligand that can be complexed with a metal. The target complex is shown below (Figure 5). It is hoped that the chirality inherent within the carbohydrate portion of this compound can be utilized to induce asymmetry as has been shown with similar catalytic compounds previously. Complexation of this ligand with various metals may lead to compounds

with a wide range of potential catalytic behaviors. The platinum derivative of this compound has the added feature of being a cisplatin analog.

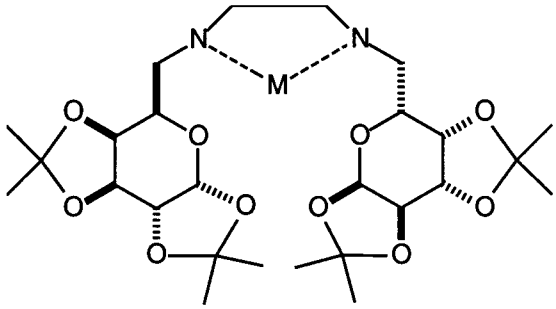

Figure 5. Target ethylene diamine ligand-metal complex

Project 1 - Results and Discussion

Synthesis of the target ligand began with 1,2:3,4-di-*O*-isopropylidene-D-galactopyranose, which is commonly known as diacetone-D-galactose (shown below, **1**). The ring carbons are conventionally numbered 1 through 5, beginning clockwise from the endocyclic oxygen. Carbon number six is the hydroxymethyl group at the top of the figure. The other six exocyclic carbons constitute the two isopropylidene protecting groups that block the hydroxyl groups normally found at carbons 1 through 4 in unmodified D-galactose. These acetals serve to prevent reaction from occurring at any

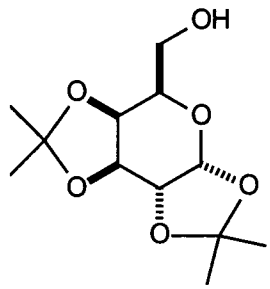

1

position save O-6, which is where the modifications to form the target compound took place.

After each synthetic step, the products were characterized mainly by NMR spectroscopy, so the correct assignment of the peaks in the ^{1}H NMR spectrum of **1** (shown below, Figure 6) became an important starting point. Furthest downfield is a small singlet at 7.26 ppm that represents residual $CHCl_3$ from the $CDCl_3$ solvent that is used in many of these NMR experiments. It will therefore show up in all of the ^{1}H NMR spectra to be described here, and will subsequently be ignored. Continuing upfield, the next signal is a doublet at 5.54 ppm. This represents the proton that is attached to the sugar ring at C-1, and is split only by the single proton at C-2. It is typical for H-1 to be

the most downfield signal in the NMR spectrum of a carbohydrate, as it is adjacent to both the endocyclic oxygen and the protected hydroxyl oxygen is that attached at the anomeric C-1. From here, things get more difficult. The remaining protons attached to the sugar ring are all adjacent to only one oxygen atom and are each two bonds removed from two more oxygen atoms. A thorough analysis of the coupling constants found in the signals from 3.6 to 4.7 ppm shows coupling between the signal at 5.54 ppm (J = 4.94 Hz), which is unambiguously known to be H-1, and the doublet of doublets found at 4.30 ppm (J = 2.38, 4.94 Hz). This signal can then be assigned to H-2. The doublet caused by splitting of H-2 by H-1 is further split into another set of doublets, as would be expected by its proximity to H-3. Coupling constant analysis again shows this to be the case, with the doublet of doublets at 4.58 ppm showing coupling constants of 2.38 and 7.87 Hz. The 7.87 Hz coupling can then be assumed to be due to splitting by H-4, whose signal appears at 4.25 ppm. Here, a splitting of 8.06 Hz is indeed found, and is within a reasonable margin of error from the expected value. What remains in the region between 3.6 and 4.7 ppm are two multiplets representing H-5, H-6 and H-6'. Even though they are on the same carbon, the two hydrogens at C-6 are in different magnetic environments, which complicates their spectrum. Coupling constants proved inconclusive for these signals, so in order to better determine H-5 from H-6 and 6', a 2-dimensional experiment

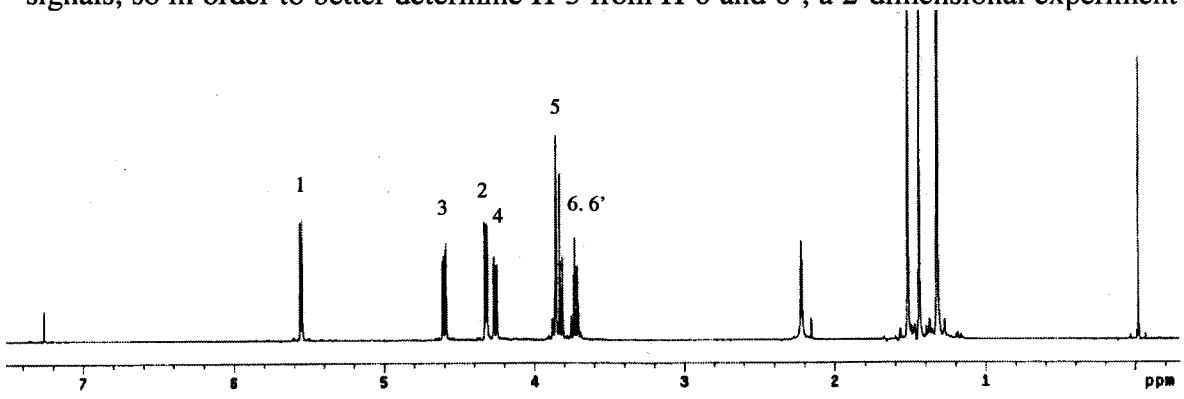

Figure 6. ^{1}H NMR of 1

known as COSY (correlation spectroscopy) was used. The results of this experiment are shown below (Figure 7). The two-dimensional experiment is interpreted as follows. Along the diagonal, from bottom left to top right, is a top-down view of the peaks of the original proton spectrum. Tracing a square from the peaks along the diagonal to the off-diagonal peaks shows coupling and/or correlation between the protons that make up the corners of the square along the diagonal. Protons H-1 through H-4 have already been assigned, and are labeled above. The dotted-line box originating at peak H-4 shows coupling with the next contour along the diagonal. These peaks, at 3.83 ppm, can therefore be assigned to H-5, while the tight square at ≈ 3.7 ppm results from H-5 coupling with H-6 and H-6'. The proton on the hydroxyl attached at C-6 is found at 2.12 ppm, and the COSY shows an unexpected correlation between this proton and H-3. This can be explained by a system in which the C-6 hydroxyl is oriented across the sugar ring, associating with H-3 in a pseudo-five membered ring conformation. The only remaining

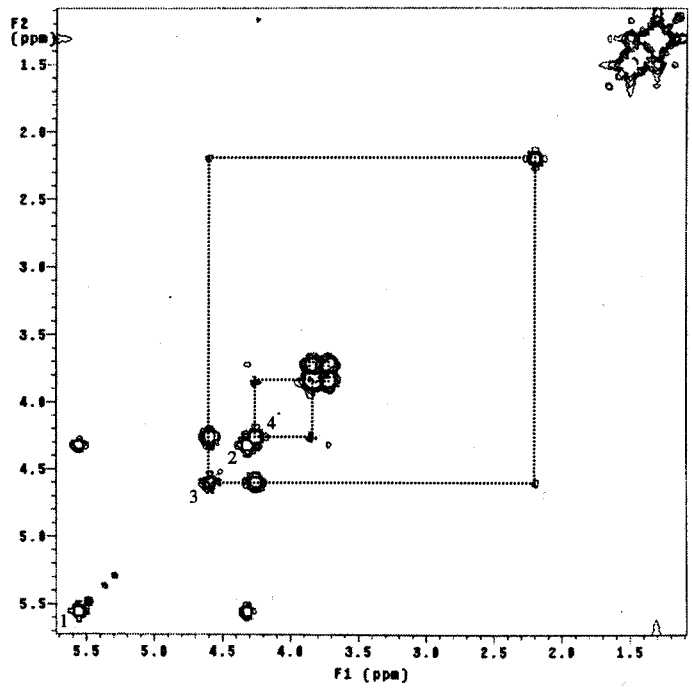

Figure 7. COSY Spectrum of 1,2:3,4-di-*O*-isopropylidene-D-galactopyranose

peaks in the spectrum are those belonging to the isopropylidene protecting groups, which fall between 1.30 and 1.50 ppm. Four of these singlets are expected, but two of these often appear as a 6 proton singlet at ≈ 1.30 ppm. Later, all four of these peaks will be evident.

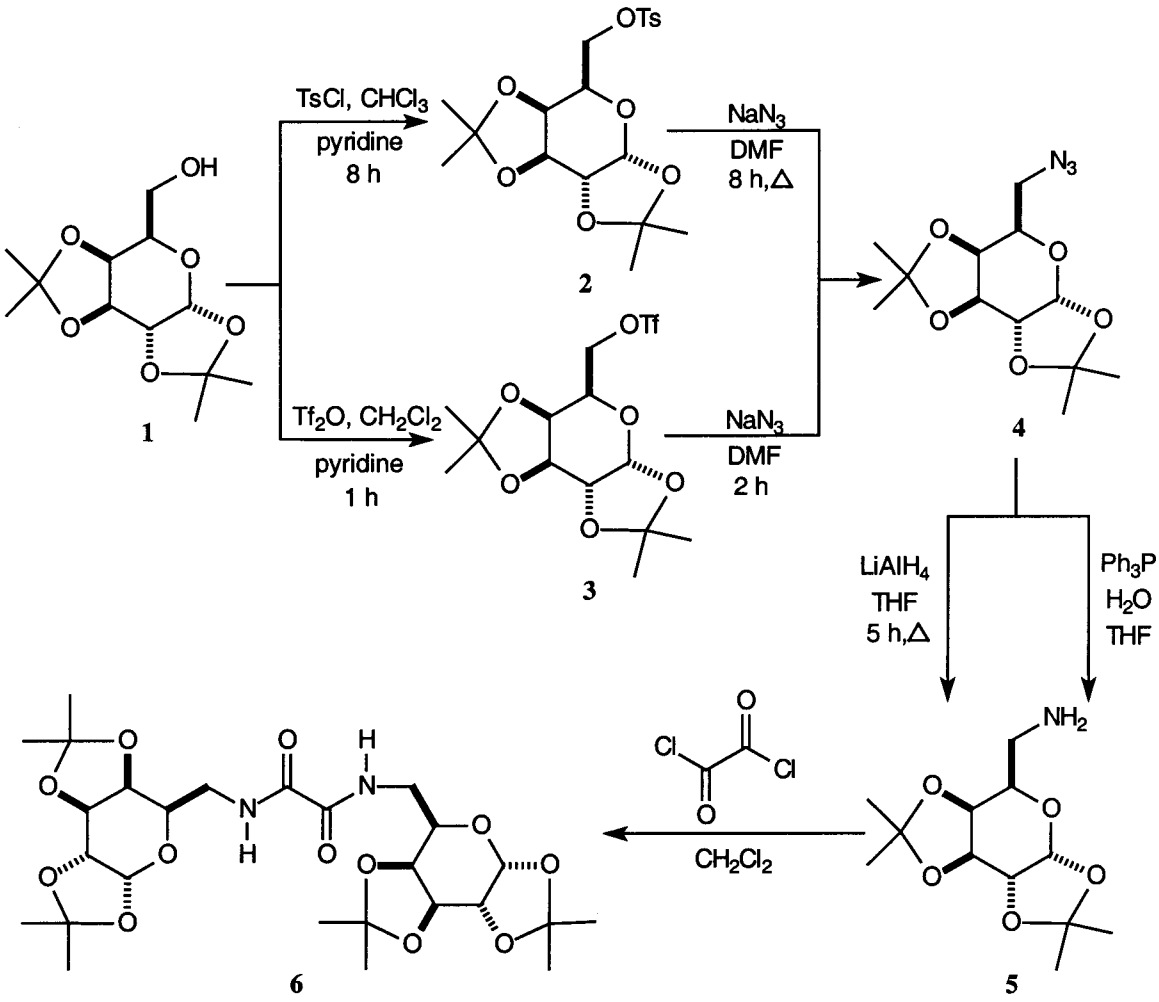

Scheme 1

Modification of diacetone galactose began with the substitution of the C-6 hydroxyl for a better leaving group (Scheme 1). Two different reagents were used for this substitution, with varying results. The first choice of reagent was *p*-toluenesulfonyl

chloride, more commonly known as tosyl chloride. Displacement of the chlorine by the sugar hydroxyl generates the moderately reactive galactose-derived tosylate shown above (Scheme 1, **2**) in ≈ 75% yield. As noted, however, this reaction took on the order of 8 h to reach completion. The second reagent used to put a leaving group at C-6 was trifluoromethanesulfonic anhydride. In a much quicker (1 h) reaction, the highly reactive triflate leaving group was placed at C-6, generating the galactose derived triflate (Scheme 1, **3**) in much better yield (94%). Each of these conversions would be expected to shift the ^{1}H NMR signal corresponding to H-6, 6' downfield, and this is indeed what is observed (Figure 8). The signals for H-6 and 6' can be found in **2** between 4.0 and 4.2 ppm, and in **3** between 4.5 and 4.6 ppm, demonstrating the greater electron withdrawing potential of the triflate group.

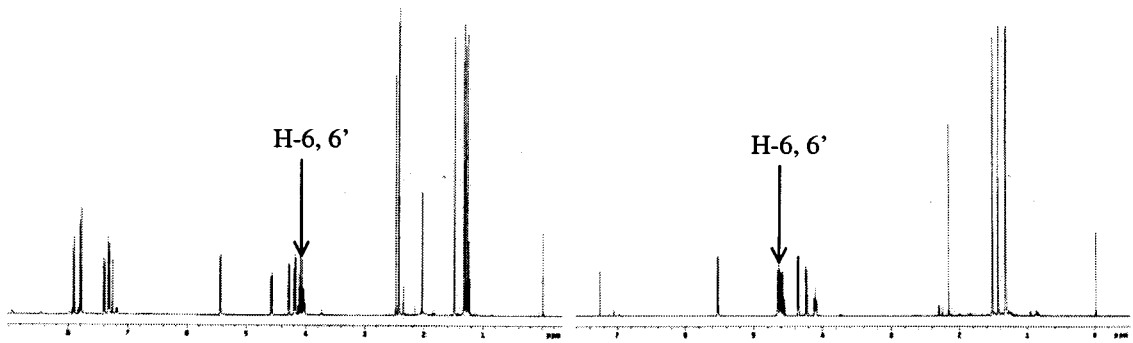

^{1}H NMR spectrum of **2** ^{1}H NMR spectrum of **3**

Figure 8

The next step was to displace the newly attached leaving group with the azide nucleophile, which was introduced by way of sodium azide. Azidation of tosylate **2** required overnight reflux in DMF (b.p. 153 °C) yielding only 60% of compound **4**, while the triflate (**3**) reacted readily at room temperature in under 1.5 hours in the same solvent, with a yield of 92% (Scheme 1). The efficiency of the triflate system in both the triflation and azidation steps led to its being the method of choice in subsequent

azidations of galactose, despite the fact that the triflic anhydride reagent is many times more expensive than tosyl chloride.

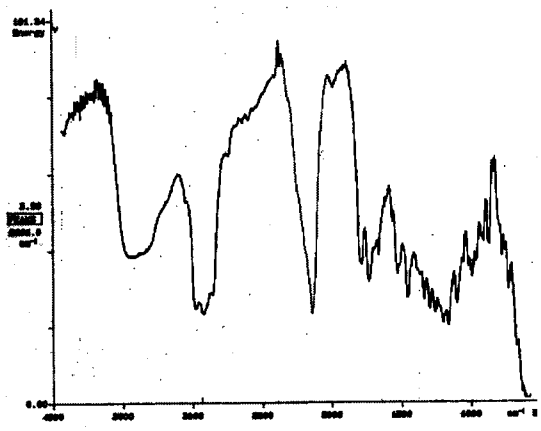

IR spectrum of **4**

A

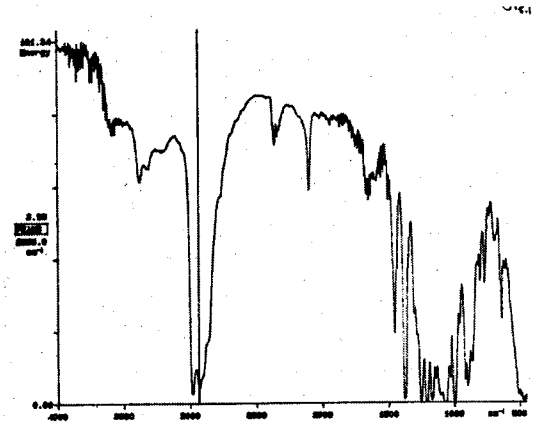

IR spectrum of **5**

B

Figure 9

The azide functionality introduced in compound **4** lends itself well to characterization not only by NMR, but also by IR spectroscopy, with a distinctive stretch at ≈ 2100 cm^{-1} (Figure 9A). Figure 9B is the IR spectrum of the reduction product of **4**, which was afforded in one of two ways. The Staudinger azide reduction protocol calls for the azide to be stirred at room temperature for 8 hours in a THF solution of 1.1 eq each of triphenyl phosphine and water (Scheme 1). However, this method proved to be troublesome in this case because the byproduct triphenylphosphine oxide was difficult to separate from the product, even *via* flash column chromotography. More useful was a standard lithium aluminum hydride reduction (Scheme 1), in which byproducts were readily removed from the crude reaction mixture by "salting" them out with dilute ammonium chloride solution followed by filtration. The ^1H NMR spectrum of reduction product **5** showed the expected shift in the signals representing H-6 and 6', and further proved that little if any byproduct contaminated the yellow-brown syrup.

Once isolated, the galactose-derived amine **5** was ready for the key step of the synthesis, which is a dimerization of **5** with oxalyl chloride to form novel diamide **6** (Scheme 1). The ^{1}H NMR spectrum of **6** (shown below, Figure 10) demonstrated the electron withdrawing influence of the newly introduced carbonyl groups on the H-6 and 6' signals, which were shifted from 2.89 ppm in the amine to 3.50 ppm in the diamide. ^{13}C NMR showed only 13 signals for the 26-carbon product, indicating that the two sugar constituents of the dimer are equivalent to each other, with one of those signals occurring at 160 ppm, indicating the presence of carbonyl functionality (Figure 10). Recrystallization of the white solid **6** yielded crystals that appeared under light microscopy to be viable for characterization *via* X-ray crystallography, so a sample was mounted and scanned for diffraction.[8] When diffraction was observed, the crystal was submitted for data collection for a period of about one week, over which time 10,000 scans of data were collected. Analysis of this data showed an extremely large unit cell, but exact locations of atoms could not be determined. It was thought that this was due to the small size of the crystal, though larger crystals were difficult to grow.

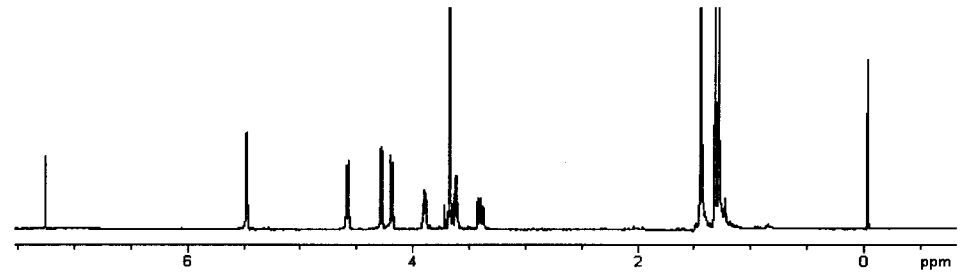

^{1}H NMR of **6**

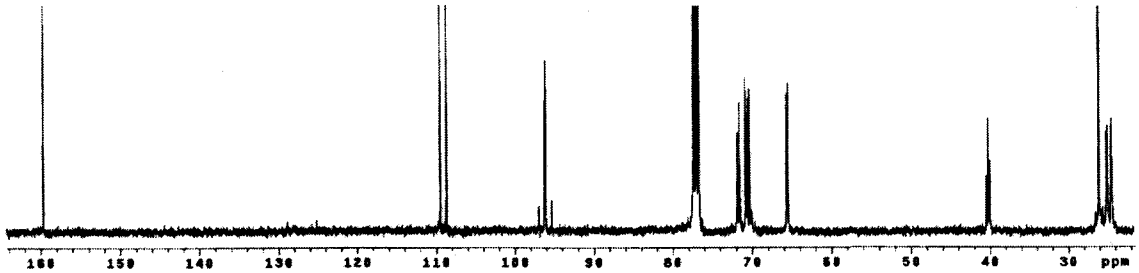

^{13}C NMR of **6**

Figure 10

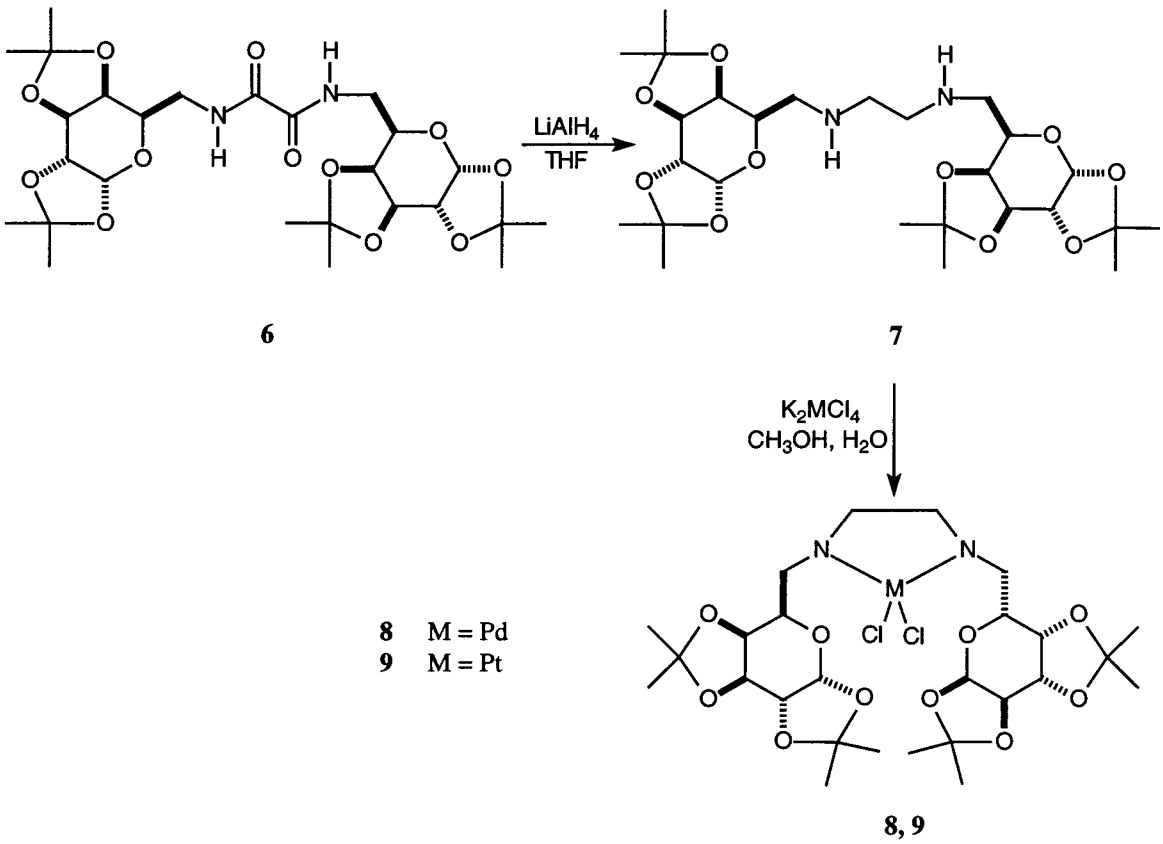

6 7 8, 9

Scheme 2

Diamide **6** needed only to be reduced in order to reach the target ligand. The reagent chosen for this transformation was lithium aluminum hydride, which is a powerful agent for the reduction of carbonyl compounds to their corresponding alkyl derivatives. The diamide proved only moderately reactive to the excess LAH to which it was subjected, and required several hours in refluxing THF in order to completely react (Scheme 2). As with amine **5**, byproducts could be removed from the reaction mixture by salting out, again with dilute ammonium chloride solution, and rotary evaporation of the filtered reaction mixture yielded the novel target ethylene diamine (**7**) as a yellow syrup. The ^{1}H NMR spectrum of **7** showed signals H-6 and 6' shifted back upfield to around 2.80 ppm, proving the removal of the electron withdrawing influence of the carbonyl groups from the diamide starting material, while the ^{13}C spectrum also showed no sign of the carbonyl signals at 160 ppm (Figure 11). As the goal of the synthesis was

to create a chiral ligand, compound **7** was tested for optical activity, and was shown to have an $[\alpha]_D$ of –54.9°.

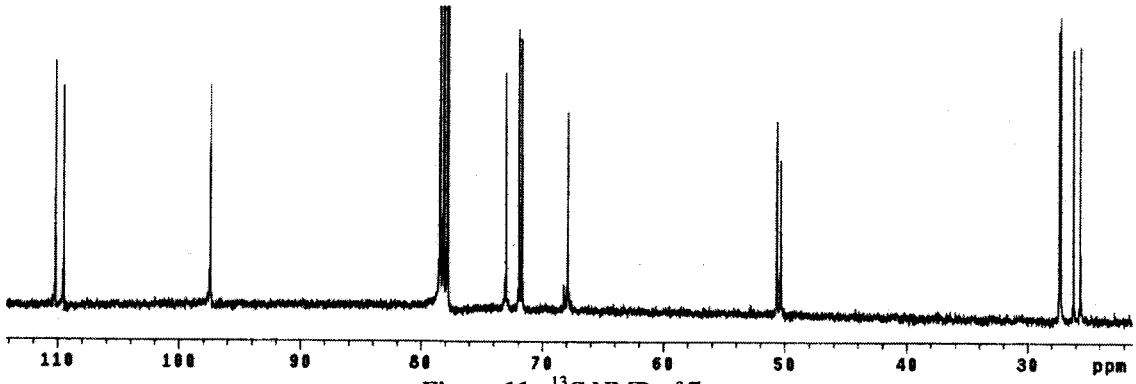

Figure 11. ^{13}C NMR of **7**

With ethylene diamine **7** in hand, tests for coordination with various metals could begin. To this end, a methanolic solution of **7** was added to a solution of anhydrous cobalt (II) chloride in methanol, which by itself has a purplish-blue color. The resulting solution immediately turned green, which was preliminary evidence of the complexation ability of the ligand. Further evidence of this reaction was appearance of a shoulder in the UV-Vis spectrum at 324 nm that represents the change in the electronic structure of the metal caused by the coordination of the ligand. Next, the spotlight was turned to more useful derivatives of this complex, utilizing palladium and platinum as the metal component. Chiral palladium complexes of this sort (Scheme 2, **8**) could potentially serve as asymmetric hydrogenation catalysts, while the platinum derivative (Scheme 2, **9**) is an analog of the cancer-fighting compound cisplatin, shown below (Figure 12). Each of these compounds was readily synthesized by introducing the metal as a potassium tetrachloride salt. The ligand readily and quickly displaces two of the chlorines, forming a precipitate that immediately crashes from the ethanol/water solution. Subsequent workup yields each of the product complexes as a yellow solid that is soluble in most

common organic solvents.

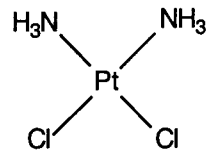

Figure 12. Cisplatin

Initial characterization on these complexes was done *via* NMR spectoscopy, where the spectra now show not one, but two magnetic environments for each of the protons on the sugar moieties (Figure 13). This is to be expected if coordination with the metal "locks" the ligand into an unsymmetric conformation, and is most obvious with regards to the H-1 doublets at 5.45 and 5.61 ppm. In addition, the complexes were tested for optical activity, with the palladium derivative exhibiting $[\alpha]_D$ = -32.9°, and the platinum derivative showing a rotation of $[\alpha]_D$ = -5.1°. After many attempts to recrystallize these compounds from various solvent systems, leaving a solution of complex **8** in ethyl acetate/hexane to slowly evaporate finally grew crystals that were amenable to single crystal X-ray diffraction analysis. The results of this proved conclusively that the bidentate ligand had indeed displaced two chlorines from the metal salt and formed a complex that was square planar about the metal center (Figure 14).

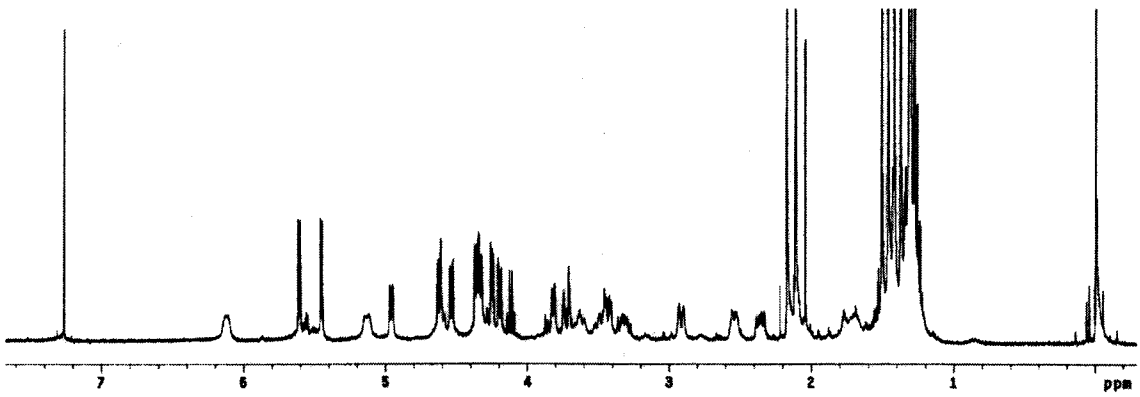

Figure 13. ^{1}H NMR of **8**

The results of this project were presented at the 217th National Meeting of the American Chemical Society in Anaheim, CA. Future work on this project will most likely proceed in two directions. One will focus on enhancing the rigidity of the ligand/metal complex, perhaps by developing a tetradentate sugar-derived ligand. The second will be to test the product compounds for their ability to induce asymmetry into a prochiral substrate and for catalytic activity in these reactions.

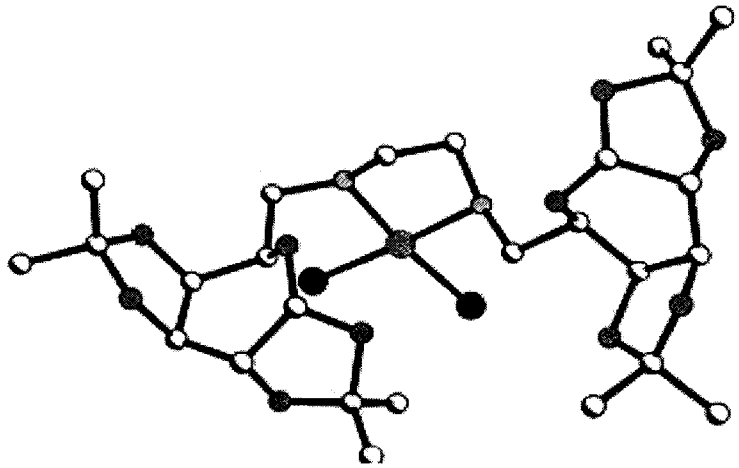

Figure 14. X-ray Crystal Structure of **8**

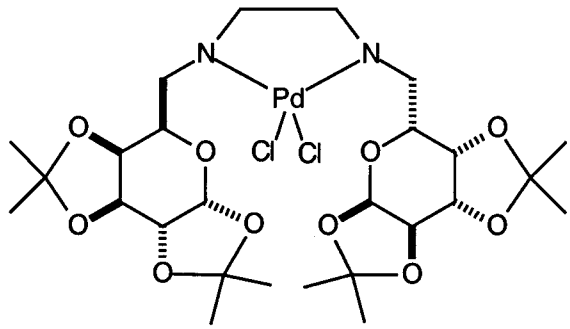

8

Project 2 - Introduction

The development of new techniques for the efficient synthesis of complex, bioactive molecules is another driving force in organic chemistry. Traditionally, organic chemical reactions involve dissolving one or more reagents in a suitable solvent, under conditions (stirring, heat, light, etc.) which favor reaction of those reagents. At the conclusion of reaction, the product(s) must then be separated not only from the solvent, but also from any remaining starting material and any byproducts that may have been formed along the way. The product must then be verified as the desired one using any of several means of characterization now available to chemists. This description may sound trivial. However, when the target compound is many steps removed from the starting materials, or when many new compounds are desired in a relatively short period of time, efficiency of reaction, purification, characterization, time management and cost at each step become of utmost importance. Many methods have been developed to bolster the efficiency of one or more of these critical components of chemical synthesis. However, very often there is a trade-off when doing this. For example, in order to promote full reaction of starting materials to products in a bimolecular reaction, one could increase the concentration of one of the reagents. Doing so, however, could lead to increased difficulty in the purification step of the synthesis. Alternatively, column chromotography is an excellent method for purification of a mixture of products, but has the downfall of being a time-consuming process. A most desirable technique would tackle all of these critical sub-problems at once.

A major step toward this end was the development of solid-phase organic synthesis. In 1963, Merrifield and co-workers used a chloromethylated-polystyrene as a

support for a protected amino acid. This polymer-bound amino acid was then deprotected and coupled with new protected amino acids. This was followed by several more rounds of the same deprotection/addition process, which eventually formed a polypeptide chain. The beauty of this system is the ease of purification it allows. Byproducts and excess reagents can be removed easily and quickly from the polymer-bound product at each step simply by washing and rinsing the resin beads.[9] This technique also allows the use of large reagent excesses to drive reactions to completion.[10] This solid-phase technique has since gone through many iterations, and has found myriad new applications. Relatively recent literature describes solid-phase Diels-Alder cycloadditions,[12] aldol condensations,[13] and Wittig reactions[13] to name a few. The number of reaction types to which this method can now be applied is enormous.

An even more recent application of solid-phase methods is in the field of combinatorial chemistry. Combinatorial chemistry is a means for the "rapid synthesis of large, organized collections of (related) compounds."[14] Solid-phase synthesis provides an accessible route to such large libraries. As an example, one can consider the synthesis of polypeptides. A first amino acid is bound to a solid resin. This resin is then divided into, for example, twenty wells. To each of these wells are added a second amino acid, which is different in each well. The result is twenty different dipeptides. Each of these polymer-bound dipeptides are then filtered from the reaction mixture, washed, and divided into twenty more wells. To each of these is added a third amino acid, again different in each well. The product of this round of synthesis is then 20x20 or 400 different tripeptides. Another round of reaction would result in 400x20 or 8000 tetrapeptides. A diagram of the combinatorial strategy is shown below (Scheme 3).[15]

Because each round of filtration and washing is quick, as well as readily automated, one can quite easily generate libraries of tens of thousands of compounds in short order. Such proficiency in such a short time by solution-phase methods would require many organic chemists. These advantages are making combinatorial chemistry one of the "hottest" areas in chemistry today. References found on the World Wide Web[16] point to more than 1800 articles published in the field in 1997 and 1998 alone.

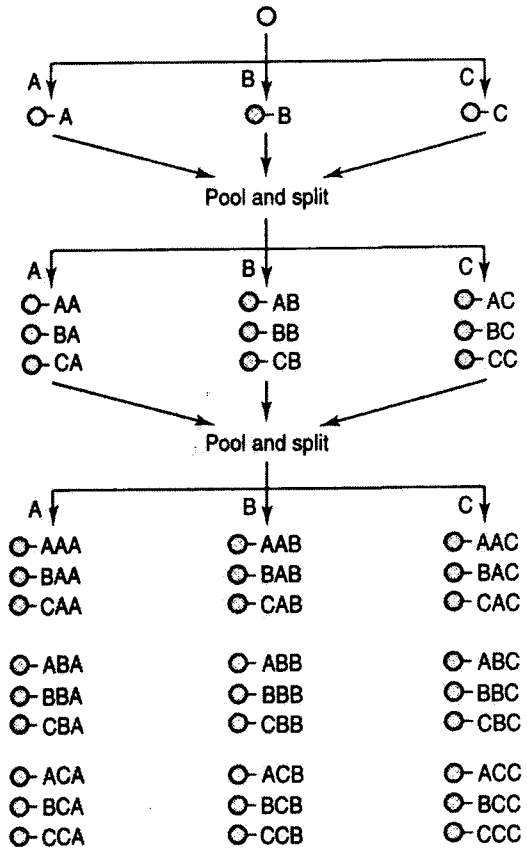

Scheme 3

Despite the utility and versatility of the solid phase method, it too has its tradeoffs. The first of these is heterogeneity. Standard solution-phase chemistry involves a relatively homogeneous solution of the reactants, and interactions between them are governed by standard diffusion and solvation principles. On the other hand, a resin-bound substrate is a tiny, partially solvated entity attached to a relatively enormous

insoluble polymeric bead. The interactions of such a substrate with the reactants in solution are therefore significantly limited, leading to consequences such as decreased overall reactivity and altered chemo- or regio-selectivity. A second major disadvantage of solid-phase based systems is the difficulty in characterization of polymer-bound products. NMR spectroscopy, one of the mainstays of organic structural analysis, is difficult to impossible with the heterogeneous environment of resin-bound compounds, though this is an area where advances are being made. Modified experiments in IR or MS can be used in the characterization of such compounds, though these techniques are not routine.[17] To combat the disadvantages of the solid-phase method, while keeping intact the advantages of polymer-supported synthesis, yet another method has been developed. The use of polymer supports that are completely soluble in most (but not all) organic solvents is showing increasing utility in this capacity. Advantages of such a system are manifold: problems with decreased reactivity due to heterogeneity are eliminated; the characterization of intermediates *via* NMR is now straightforward; ease of purification is comparable to that of solid-phase methods. While solid-phase systems utilize an easy to filter bead, the bulk properties of the soluble polymer are such that it may be easily precipitated from solution and filtered. This allows the use of large reagent excesses to drive reactions to completion, which requires only that the product be easily separable from the reaction mixture. Combinatorial synthesis is then readily performed on soluble polymer-bound substrates.

This soluble polymer, or "liquid-phase" method has been applied to many areas of organic synthesis, including peptide synthesis,[18] oligonucleotide synthesis,[19] and oligosaccharide synthesis.[20] Far from being limited to oligomeric molecules, the liquid-

phase method is applicable to many synthetic systems. The only requirements for its use are a) the presence of a point of attachment for the polymer on the substrate and b) the means to link the substrate to the polymer that is at once stable to all the reaction conditions to which it will be subjected and easy is to cleave when the time comes. The current research will focus on the synthesis of carbohydrate-derived heterocyles using this liquid-phase methodology. With their multiple hydroxyl groups as potential points of attachment, carbohydrate derivatives make excellent substrates for polymer-supported chemistry.

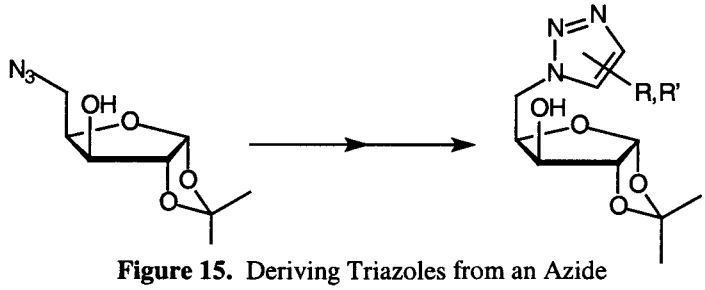

Figure 15. Deriving Triazoles from an Azide

As mentioned previously, azide intermediates are also a "theme" of the current research. In this case, the 5-deoxy-5-azido derivative of 1,2-*O*-isopropylidene-D-xylofuranose (Figure 15) will be used *en route* to nucleoside analogs. Nucleosides in nature consist of a carbohydrate bound at C-1 to a nitrogen-containing heterocycle. A number of nucleoside mimics have been found to demonstrate significant antiviral activity, including the herpes drugs acyclovir[21] and 5,5,5-trifluorothymidine,[22] and the HIV inhibitor 3'-deoxy-3'-azidothymidine[23] (Figure 16). This research concerns the synthesis of analogs in which the heterocyclic group is placed at the C-5 position of the sugar, rather than the anomeric position. These compounds are termed "reversed nucleoside analogs," and several examples of such compounds have previously been synthesized in good to high yield.[24] This work augments the collection of these

molecules, while at the same time providing a comparison between the solution-phase methods used in the previous work and the liquid-phase methods used here.

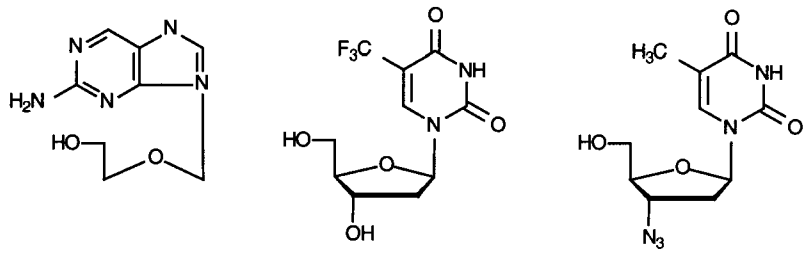

Acyclovir **5,5,5-Trifluorothymidine** **Azidothymidine**

Figure 16. Examples of Nucleoside Analogs with Antiviral Activity

Project 2 - Results and Discussion

In past studies, the compound 1,2-*O*-isopropylidene-D-xylofuranose (Scheme 4, **10**) served as the starting point in the synthesis of reversed nucleoside analogs.[24] The first step was to specifically substitute azide functionality for the primary hydroxyl group at C-5 *via* a tosylate intermediate (Scheme 4). By lowering the temperature of the tosylation step, the researchers were able to leave unreacted the secondary hydroxyl at C-3. Azide **12** then served as the dipole component in a 1,3-dipolar cycloaddition reaction in which the heterocyclic constituent of the nucleoside analog was introduced to form triazoles **13-15** (Scheme 4). Of interest here will be three specific triazoles from the previous work. The first (Scheme 4, **13**) was constructed using propargyl alcohol as the dipolarophile, the second (**14**) used ethyl propiolate, and the third (**15**), phenyl acetylene.

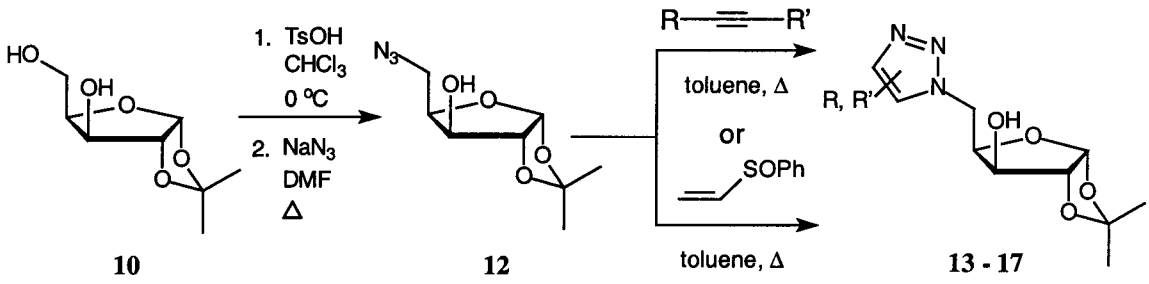

13 R = CH_2OH; R' = H
14 R = CO_2Et; R' = H
15 R = Ph; R' = H
16 R = Ph; R' = Ph
17 R = H; R' = H

Scheme 4

To expand this library of reversed nucleoside analogs, the current research utilized the dipolarophiles diphenyl acetylene to give **16** and the acetylene equivalent phenyl vinyl sulfoxide to give **17**. While the previous cycloadditions were completed in 30 hours in refluxing toluene, the current set needed more strenuous conditions in order to fully react. The diphenyl acetylene derivative, presumably due to its steric bulk,

required 3-4 days in refluxing *o*-xylene to completely react. Cycloaddition of **10** with phenyl vinyl sulfoxide, on the other hand, proceeded well in refluxing toluene, but subsequent elimination of phenyl sulfinic acid to form the parent, unsubstituted triazole seemed to require boiling xylene. In addition, purification of unsubstituted triazole **17** proved to be most difficult, as even flash column chromotography left behind significant amounts of an aromatic byproduct, assumed to be phenyl sulfinic acid. Polymer-supported chemistry would prove to be the solution to this problem.

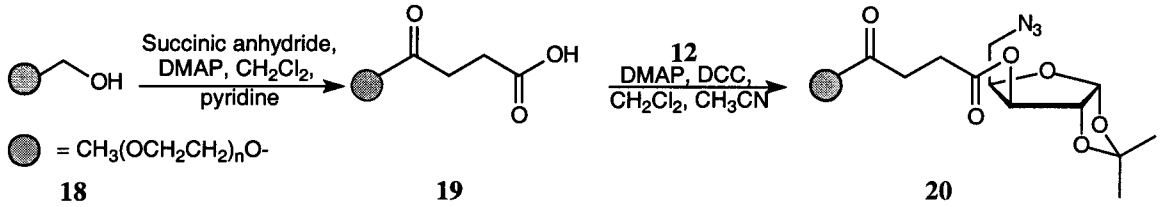

Scheme 5

In addition to expanding the library of nucleoside analogs, this research also examined the advantages of applying the soluble-polymer methodology mentioned above to their synthesis. Because of its many useful characteristics, the monomethyl ether of polyethylene glycol (MPEG) (Scheme 5, **18**) was chosen as the polymer support for this reaction sequence. Most important of these is its solubility in most common organic solvents, such as methylene chloride, chloroform, ethyl acetate, etc. This feature allows homogeneous reaction conditions, as well as characterization of synthetic intermediates by standard solution-phase NMR. MPEG is not soluble, however, in ethereal solvents, a fact that is used to advantage in the purification steps of the synthesis. A second noticeable feature of MPEG is its terminal methyl group. The ^{1}H NMR signal for this group appears at 3.35 ppm and its integral value provides an internal standard upon which to base efficiency of reaction and effective yields. A final key factor is the

terminal hydroxyl group, which serves as an anchoring point at which the substrate can be attached.

One other decision must be made before polymer-supported (liquid-phase) synthesis can take place. A linker must be found that will join the polymer to the substrate such that it is stable to all the reaction conditions it will be exposed to, while at the same time readily cleaved to allow removal of the ultimate product from the support. Based on past work in this lab, a succinate system (Scheme 5, **19**) was chosen as a viable linker. After this linker was attached, the substrate azide **12** was attached to the linker by way of a dicyclohexylcarbodiimide (DCC) coupling, which joined the carboxylic acid functionality of **19** with the free hydroxyl at C-3 in the sugar. The resulting polymer-supported dipole (Schemes 5 and 6, **20**) was now ready to undergo the same cycloadditions found in Scheme 4.

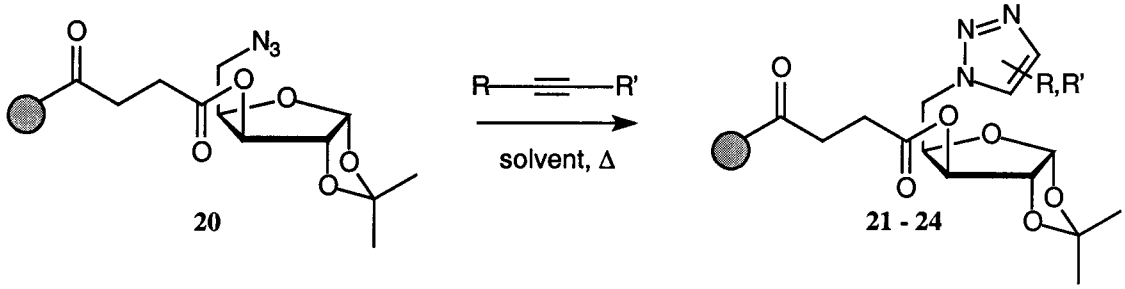

20 **21 - 24**

21 R = CH_2OH; R' = H
22 R = CO_2Et; R' = H
23 R = H; R' = H
24 R = Ph; R' = H

Scheme 6

The methodology produced very encouraging results in many cases. For example, the propargyl alcohol, ethyl propiolate, and phenyl vinyl sulfoxide derived cycloadducts (Scheme 6, **21, 22,** and **23**, respectively) were constructed on the polymer in yields greater than 95% each, as determined *via* integration of the ^1H NMR spectra of the various cycloadducts (Figure 17). This was calculated by comparing the integrals of the

signals corresponding to the triazole protons (7.5 to 8.3 ppm) to those of the internal standard terminal methyl group at 3.35 ppm. These yields were better than the solution-phase yields for the previously reported cycloadditions. Another interesting result was the regiochemical selectivity found, which is based on the two modes by which the dipolarophile can approach the dipole. In the solution-phase work, the propargyl alcohol derivatives **13** were synthesized in a 1:1 ratio, while the polymer-supported synthesis afforded a 1.7:1 ratio of the two regioisomers **21**, presumably due to the steric bulk of the polymer-supported dipole. This phenomenon was seen in the ethyl propiolate derivative **14** as well, with a solution-phase ratio of 2:1 and polymer-supported (**22**) ratio of 3:1. Strangely, the reverse outcome was seen with the phenyl acetylene derivatives, where solution-phase reaction yielded a single regioisomer **15**, whereas liquid-phase cycloaddition afforded two regioisomers **24** in a 4:1 ratio.

Using the liquid-phase method undoubtedly led to the high yields seen here, as large excesses of the dipolarophiles were used with the knowledge that the desired product could be easily removed from the reaction mixture by precipitation with ice-cold ether. This system made workup and purification somewhat quicker than would have been possible with solution-phase synthesis. The liquid-phase system was not without its caveats, though. The phenyl acetylene derivative **15**, which was synthesized in 82% yield after 20 hours in refluxing toluene, showed only 50% conversion to product after 5 days in refluxing xylene using the polymer-supported method. Along the same lines, cycloaddition between azide **12** and diphenyl acetylene in refluxing xylene allowed a modest yield of 60%, but the same reaction with polymer-bound azide **20** showed no cycloadduct whatsoever, regardless of reaction conditions.

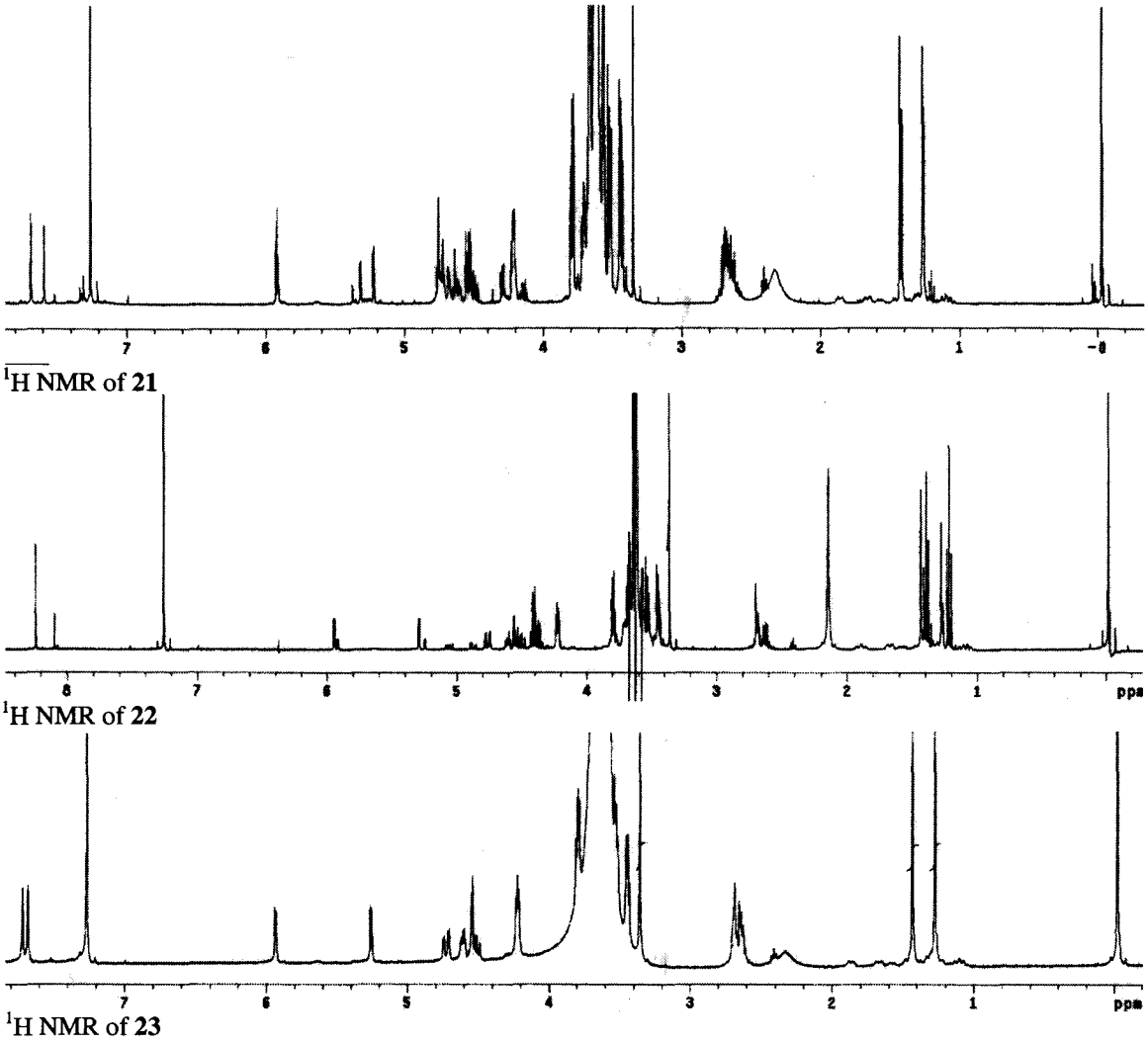

Figure 17

One remaining issue was the removal of the cycloadducts from their polymer supports, which was readily accomplished by stirring the polymer-bound triazoles in a methanolic solution of ammonia. Subsequent precipitation of the polymer followed by filtration and evaporation of the filtrate yielded a crude mixture that was then flushed through a plug of silica to yield the product triazoles at 85 to 93 percent yield. As mentioned previously, parent triazole **17** synthesized by the solution-phase method proved difficult to purify as evidenced by its NMR spectra below (Figure 18). However, the polymer-bound triazole **23** can be cleaved cleanly and purified quite easily to yield

the same product (**17**), but in much more pure form (Figure 18).

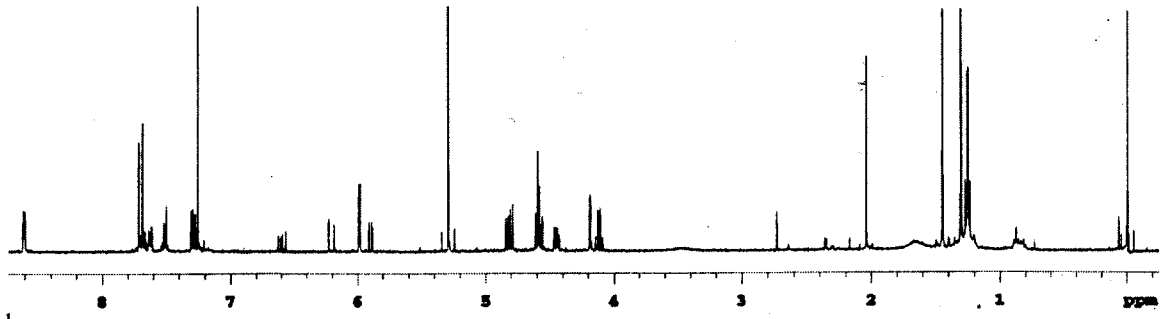

^{1}H NMR of **17** (solution-phase)

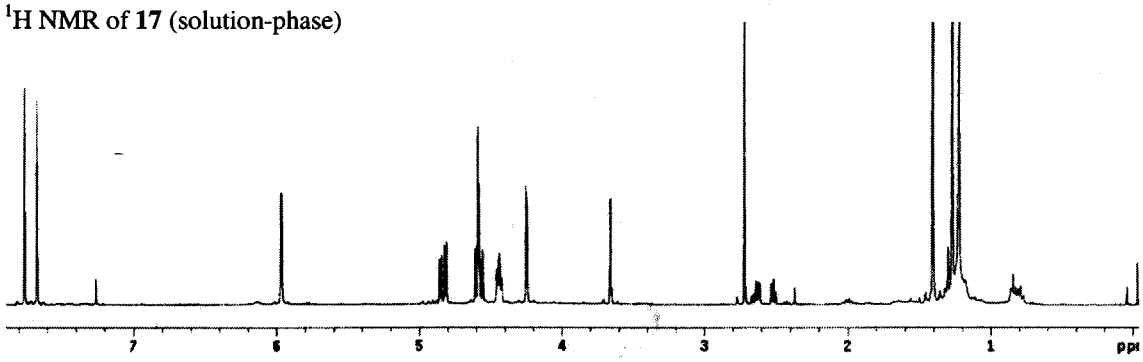

^{1}H NMR of **17** (liquid-phase)

Figure 18

This work served as this research group's introduction into the liquid-phase methodology, and future work will concentrate on two major offshoots of the current study. Many novel derivatives of the compounds synthesized here could be produced by using different polymer-mounted dipoles (nitrile oxides or nitrones, for example), by introducing different dipolarophiles, or by changing the sugar constituent. Libraries of these compounds could be synthesized quickly and readily in a combinatorial-type strategy. Separately, the liquid-phase method will be applied to the combinatorial synthesis of derivatives of known biologically active compounds in hopes of increasing activity in those systems.

Experimental

General Procedures

^{1}H and ^{13}C NMR were recorded on a Varian Gemini 2000 system at 400 and 100 MHz respectively, using $CDCl_3$ or d_6-DMSO as solvent. Proton and carbon shifts (δ) are recorded in parts per million (ppm). Multiplicities are labeled as follows: s (singlet), d (doublet), t (triplet), q (quartet), m (multiplet), with coupling constants (*J*) measured in Hertz. Infrared spectra were taken on a Perkin Elmer Model 1600 FT-IR spectrophotometer. Optical rotations were recorded on a Perkin Elmer 323 Automatic Polarimeter. Analytical thin layer chromotography was carried out on Whatman aluminum-backed flexible plates. Flash column chromotography utilized 70-270 mesh 60-Å silica gel.

Project 1

1,2:3,4-Di-*O*-isopropylidene-D-galactopyranose (1).

^{1}H NMR (δ): 5.54 (d, 1H, *J* = 4.94, H-1); 4.58 (dd, 1H, *J* = 2.38, 7.87, H-3); 4.30 (dd, 1H, *J* = 2.38, 4.94, H-2); 4.25 (dd, 1H, *J* = 1.65, 8.06, H-4); 3.82 (m, 1H, H-5); 3.73 (m, 2H, H-6, 6'); 2.12, (d, 1H, *J* = 4.58, OH - C-6); 1.50 (s, 3H, CH_3); 1.43 (s, 3H, CH_3); 1.30 (s, 6H, 2 x CH_3).

Synthesis of 1,2:3,4-di-*O*-isopropylidene-6-*O*-(*p*-tolylsulfonyl)-D-galactopyranose (2) from 1,2:3,4-di-*O*-isopropylidene-D-galactopyranose (1).

1,2:3,4-di-*O*-isopropylidene-D-galactopyranose (**1**) (2.13g, 8.18 mmol) and 5 mL pyridine were dissolved in 30 mL CH_2Cl_2 with stirring. *p*-Toluenesulfonyl chloride

(1.72g, 1.1 eq) was added and the mixture stirred overnight. Full reaction of starting material was confirmed *via* TLC using 3:1 hexane:ethyl acetate as eluent. The solution was then added to water (30 mL) and the product extracted with CH_2Cl_2 (3x25 mL). The organic phase was then washed with 5% sulfuric acid (2x25 mL), followed by water (1x25 mL). The product solution was then dried over $MgSO_4$ and concentrated under vacuum to yield the white solid tosylate (**2**), which was recrystallized from ethyl acetate/hexane with a yield of 3.38g (75%).

^{1}H NMR (δ): 7.3-7.9 (2d, 4H, phenyl ring); 5.54 (d, 1H, J = 4.94, H-1); 4.57 (dd, 1H, J = 2.57, 7.88, H-3), 4.28 (dd, 1H, J = 2.56, 4.94, H-2); 4.0-4.2 (m, 4H, H-4, 5, 6, 6'); 1.49, 1.33, 1.30, 1.27 (s, 12H, 4 x CH_3).

Synthesis of 1,2:3,4-di-*O*-isopropylidene-6-*O*-trifluoromethylsulfonyl-D-galacto-pyranose (3) from 1,2:3,4-di-*O*-isopropylidene-D-galactopyranose (1).

To a 1000 mL round-bottom flask was added 6.5 mL pyridine (2eq) and 300 mL of dry CH_2Cl_2. This solution was cooled to –10 °C. In a pressure-equalizing addition funnel, 13.37 mL triflic anhydride was dissolved in 100 mL dry CH_2Cl_2, and this solution was added dropwise to the pyridine solution. This resulted in a thick pink mixture. At the completion of addition, a solution of 1,2:3,4-di-*O*-isopropylidene-D-galactopyranose (**1**) (10.384g, 40 mmol) in 100 mL dry CH_2Cl_2 was added dropwise to the mixture. This mixture was then stirred for 2 h following the completion of addition. Full reaction of starting material was confirmed *via* TLC using 3:1 hexane:ethyl acetate as eluent. The solution was then added to 250 mL ice water and extracted 3 times with CH_2Cl_2. Combined organic phases were then washed with 5% sulfuric acid (2x100 mL), followed

by water (1x100 mL). Product solution was then dried over $MgSO_4$ and rotary evaporated under vacuum to yield a dark red to purple syrup (**3**) at 94% (14.7 g).

^{1}H NMR (δ): 5.53 (d, 1H, *J* = 4.95, H-1); 4.55-4.65 (m, 3H, H-3, 6, 6'); 4.35 (dd, 1H, *J* = 2.56, 4.94, H-2); 4.23 (dd, 1H, *J* = 2.02, 7,87, H-4); 4.10 (m, 1H, H-5); 1.52s, 1.43s, 1.32 2s (12H, 4 x CH_3).

Azidation of 1,2:3,4-di-*O*-isopropylidene-6-*O*-(*p*-tolylsulfonyl)-D-galactopyranose (2) to 6-azido-6-deoxy-1,2:3,4-di-*O*-isopropylidene-D-galactopyranose (4).

To a solution of 1,2:3,4-di-*O*-isopropylidene-6-*O*-(*p*-tolylsulfonyl)-D-galacto-pyranose (**2**) (6.27g, FW=414, 15.1 mmol) in 250 mL DMF was added NaN_3 (2.95g, 3 eq). This mixture was stirred at reflux overnight, after which time full reaction of starting material was confirmed *via* TLC using 3:1 hexane:ethyl acetate as eluent. This was followed by filtration of unreacted NaN_3 and vacuum evaporation of the solvent. The resulting residue was dissolved in CH_2Cl_2 (50 mL), and added to 50 mL water. This was extracted with CH_2Cl_2 (3x50 mL), decolorized with charcoal, dried over $MgSO_4$ and vacuum evaporated. This resulted in brown syrup (**4**) in an overall yield of 2.6 g (60%).

^{1}H NMR (δ): 5.53 (d, 1H, *J* = 5.12, H-1); 4.61 (dd, 1H, *J* = 2.56, 7.87, H-3); 4.32 (dd, 1H, *J* = 2.56, 5.13, H-2); 4.17 (dd, 1H, *J* = 1.83, 7,87, H-4); 3.9 (m, 1H, H-5); 3.4 (m, 2H, H-6,6'); 1.53s, 1.44s, 1.33s, 1.32s (12H, 4 x CH_3).

Azidation of 1,2:3,4-di-*O*-isopropylidene-6-*O*-trifluoromethylsulfonyl-D-galacto-pyranose (3) to 6-azido-6-deoxy-1,2:3,4-di-*O*-isopropylidene-D-galactopyranose (4).

To a solution of 1,2:3,4-di-*O*-isopropylidene-6-*O*-trifluoromethylsulfonyl-D-galactopyranose (**3**) (10.9g, FW=392, 28 mmol) in 200 mL DMF was added NaN_3 (4.67g, 2.5 eq). The mixture was stirred for 2-3 h. Full reaction of starting material was confirmed *via* TLC using 3:1 hexane:ethyl acetate as eluent. Unreacted NaN_3 was filtered, and the solvent was removed by vacuum evaporation. The resulting residue was dissolved in CH_2Cl_2 (50 mL), and added to 50 mL water. This was extracted with CH_2Cl_2 (3x50 mL), dried over $MgSO_4$ and vacuum evaporated. This resulted in a brown syrup (**4**) in an overall yield of 7.34 g (92%).

^{1}H NMR (δ): 5.53 (d, 1H, *J* = 5.12, H-1); 4.61 (dd, 1H, *J* = 2.56, 7.87, H-3); 4.32 (dd, 1H, *J* = 2.56, 5.13, H-2); 4.17 (dd, 1H, *J* = 1.83, 7.87, H-4); 3.9 (m, 1H, H-5); 3.4 (m, 2H, H-6,6'); 1.53s, 1.44s, 1.33s, 1.32s (12H, 4 x CH_3).

Staudinger reduction of 6-azido-6-deoxy-1,2:3,4-di-*O*-isopropylidene-D-galacto-pyranose (4) to 6-amino-6-deoxy-1,2:3,4-di-*O*-isopropylidene-D-galactopyranose (5).

To a solution of 6-azido-6-deoxy-1,2:3,4-di-*O*-isopropylidene-D-galactopyranose (**4**) (1.2 g, FW=285, 4.5 mmol) in 20 mL THF was added triphenyl phosphine (1.33g, 1 eq) along with 0.1 mL of H_2O. This mixture was stirred overnight, followed by filtration of triphenylphosphine oxide byproduct. TLC using pure ethyl acetate as solvent showed product at baseline as well as a less polar, UV active spot that proved to be yet more triphenylphosphine oxide. This byproduct proved difficult to remove, even *via* flash column chromotography, and finally a crude yield of 0.76 g (65%) was obtained for the product amine.

^{1}H NMR (δ): 5.55 (d, 1H, *J* = 4.94, H-1); 4.58 (dd, 1H, *J* = 2.38, 8.06, H-3); 4.30 (dd, 1H, *J* = 2.20, 4.94, H-2); 4.21 (dd, 1H, *J* = 1.83, 7.87, H-4); 3.69 (m, 1H, H-5); 2.89 (m, 2H, H-6,6'); 1.52s, 1.44s, 1.32ss (12H, 4 x CH_3).

Lithium aluminum hydride reduction of 6-azido-6-deoxy-1,2:3,4-di-*O*-isopropylidene-D-galactopyranose (4) to 6-amino-6-deoxy-1,2:3,4-di-*O*-isopropylidene-D-galactopyranose (5).

A solution of 6-azido-6-deoxy-1,2:3,4-di-*O*-isopropylidene-D-galactopyranose (6.0g, FW=285, 21 mmol) in 200 mL dry THF was cooled to -10° C. In small portions, lithium aluminum hydride (2.46g, 3 eq) was added. The resulting mixture was heated to ≈ 60 °C, and stirred overnight, at which time TLC using pure ethyl acetate as eluent showed complete conversion of starting material. Excess LAH was then quenched with a saturated solution of ammonium chloride, added dropwise until no further reaction (i.e. bubbling) occurred upon its addition. The resulting salts were filtered from the solution, and the filtrate was evaporated under vacuum to yield the amine product in 70-75% (≈ 3.8 g).

^{1}H NMR (δ): 5.55 (d, 1H, *J* = 4.94, H-1); 4.58 (dd, 1H, *J* = 2.38, 8.06, H-3); 4.30 (dd, 1H, *J* = 2.20, 4.94, H-2); 4.21 (dd, 1H, *J* = 1.83, 7.87, H-4); 3.69 (m, 1H, H-5); 2.89 (m, 2H, H-6,6'); 1.52s, 1.44s, 1.32s, 1.33s (12H, 4 x CH_3).

Reaction of 6-amino-6-deoxy-1,2:3,4-di-*O*-isopropylidene-D-galactopyranose (5) with oxalyl chloride to form compound 6.

To a solution of 6-amino-6-deoxy-1,2:3,4-di-*O*-isopropylidene-D-galactopyranose (3.2g, FW=259, 12.3 mmol) in 100 mL dry THF was added 5 mL pyridine with stirring. A solution of oxalyl chloride (0.54 mL, 0.5 eq) in 20 mL THF was prepared in an addition funnel and added dropwise to the sugar solution and stirred for 3 h. TLC using 3:1 ethyl acetate:hexane showed complete reaction of starting materials. The reaction mixture was evaporated, redissolved in CH_2Cl_2, and added to water (50 mL). This was extracted with CH_2Cl_2 (3x25 mL), dried over $MgSO_4$, and evaporated under vacuum, to yield the product diamide **6** in 86% (6.05 g).

^{1}H NMR (δ): 5.50 (d, 1H, *J* = 4.94, H-1); 4.59 (dd, 1H, *J* = 2.38, 7.87, H-3); 4.29 (dd, 1H, *J* = 2.56, 5.13, H-2); 4.21 (dd, 1H, *J* = 2.01, 8.05, H-4); 3.91 (m, 1H, H-5); 3.5 (m, 2H, H-6,6'); 1.47s, 1.37s, 1.30s, 1.31s (12H, 4 x CH_3).

^{13}C NMR (δ): 159.68, 109.51, 108.69, 96.28, 96.10, 71.81, 71.57, 70.82, 70.75, 70.51, 70.30, 65.70, 65.48, 40.45, 40.24, 40.13, 26.10, 25.13, 25.03, 24.54, 24.46.

Reduction of diamide 6 to diamine 7.

A solution of diamide **6** (2.3 g, FW=572, 4.0 mmol) in 100 mL THF was cooled to -10°C. Slowly, in small portions, lithium aluminum hydride (850 mg, 5 eq) was added with stirring. This mixture was heated to reflux, and stirred overnight, at which point TLC using pure ethyl acetate as eluent showed complete reaction. The reaction mixture was quenched with a saturated solution of NH_4Cl added dropwise until no further reaction occurred upon its addition. The mixture was then gravity filtered, the solid

washed with CH_2Cl_2, and the combined filtrates evaporated under vacuum to yield diamine **7** as a yellow syrup in 70% (1.52 g).

^{1}H NMR (δ): 5.20 (d, 1H, *J* = 5.13, H-1); 4.57 (dd, 1H, *J* = 2.01, 7.87, H-3); 4.29 (dd, 1H, *J* = 1.65, 4.39, H-2); 4.19 (dd, 1H, *J* = 1.09, 7.87, H-4); 3.89 (m, 1H, H-5); 2.80 (m, 2H, H-6,6'); 1.52s, 1.43s, 1.32s, 1.31s (12H, 4 x CH_3).

^{13}C NMR (δ): 110.79, 109.50, 97,45, 73.00, 71.93, 71.69, 67.90, 50.65, 50.32, 27.36, 27.24, 26.19, 25.61.

Complexation of ethylene diamine ligand with palladium, platinum to form 8 and 9

Platinum: Diamine **7** (188 mg, FW=572, 0.33 mmol) was dissolved in 10 mL absolute EtOH with stirring. To this was added a solution of potassium tetrachloroplatinate (139 mg, FW=415, 0.33 mmol) in 5 mL of distilled water. The mixture was stirred overnight, followed by rotary evaporation *in vacuo* to yield a yellow-brown solid. This solid was dissolved in ethyl acetate and the remaining solid byproduct filtered. Ethyl acetate was then evaporated to yield yellow solid **9** in 84% (0.204 g).

Palladium: 177 mg of ligand (FW=572, 0.31 mmol) was dissolved in 10 mL absolute EtOH with stirring. To this was added a solution of potassium tetrachloroplatinate (102 mg, FW=326.4, 0.31 mmol) in 5 mL of distilled water. This mixture was stirred overnight, followed by rotary evaporation *in vacuo* to yield a yellow-brown solid. This solid was dissolved in ethyl acetate and the remaining solid byproduct filtered. Ethyl acetate was then evaporated to yield yellow solid **8** in 68% (0.12 g)

^{1}H NMR (δ): 5.61 (d, 1H, J = 5.31, H1); 5.45 (d, 1H, J = 4.94, H1'); all other protons are complex multiplets.

X-Ray Crystal Data for Palladium Complex 8

Table 1. Crystal data and structure refinement for tolfrz.

Identification code	Freeze	
Empirical formula	$C_{26}\ H_{42}\ C_{12}\ N_2\ 0_{10}\ Pd$	
Formula weight	719.92	
Temperature	566(2) K	
Wavelength	0.71073 Å	
Crystal system	orthorhombic	
Space group	$P2_{12121}$	
Unit cell dimensions	a = 13.638(2) Å	alpha = 90°
	b = 22.156(3) Å	beta = 90°
	c = 23.699(3) Å	gamma = 90°
Volume, Z	7161.0(15) $Å^3$, 8	
Density (calculated)	1.336 Mg/m^3	
Absorption coefficient	0.716 mm^{-1}	
F(OOO)	2976	
Crystal size	0.24 x 0.06 x 0.05 mm	
9 range for data collection	2.28 to 29.97°	
Limiting indices	$-19 \le h \le 17, -30 \le k \le 29, -32 \le l \le 30$	
Reflections collected	52487	
Independent reflections	18916 (R_{int} = 0.2699)	
Refinement method	Full-matrix least-squares on F^2	
Data / restraints / parameters	18916 / 0 / 739	
Goodness-of-fit on F 2	0.663	
Final R indices [I>2σ(I)]	Rl = 0.0607, wR2 = 0.1298	
R indices (all data)	R1 = 0.3377, wR2 = 0.2213	
Absolute structure parameter	0.01(5)	
Largest diff. peak and hole	0.399 and -0.348 e $Å^{-3}$	

Table 2. Atomic coordinates [x 10^4] and equivalent isotropic displacement parameters [$Å^2$ x 10^3]. U(eq) is defined as one third of the trace of the orthogonalized U_{ij} tensor

	x	y	z	U(eq)
Pd(1)	-1994(1)	-7106(1)	-7351(1)	61(1)
Cl(1A)	-3458(2)	-7473(2)	-6991(2)	76(1)
Cl(1B)	-2242(2)	-7550(2)	-8225(2)	72(1)
O(1A)	75(12)	-8277(9)	-6515(13)	222(11)
O(1B)	1713(7)	-5695(4)	-8391(4)	75(3)
O(2A)	-1056(17)	-8940(6)	-6328(10)	191(8)
O(2B)	1934(7)	-6320(3)	-9127(3)	64(2)
O(3A)	-1367(24)	-8433(10)	-4862(15)	250(15)
O(3B)	3064(7)	-7440(4)	-8250(4)	69(2)
O(4A)	-2250(16)	-7634(6)	-5069(7)	210(9)
O(4B)	1632(7)	-7893(4)	-8056(4)	88(3)
O(5A)	-512(17)	-7614(8)	-5886(9)	193(9)
O(5B)	1493(6)	-6560(4)	-7838(4)	60(2)
N(1A)	-1638(9)	-6667(5)	-6591(4)	70(3)
N(1B)	-715(7)	-6722(4)	-7656(4)	61(3)
C(1A)	-77(40)	-8128(22)	-5942(26)	375(40)
C(1B)	2157(9)	-6220(6)	-8153(6)	58(4)
C(2A)	-700(17)	-8760(10)	-5764(17)	154(11)
C(2B)	2564(9)	-6537(5)	-8682(6)	54(4)
C(3A)	-1629(39)	-8583(13)	-5495(16)	244(18)
C(3B)	2415(10)	-7225(6)	-8671(6)	61(4)
C(4A)	-2232(19)	-7977(9)	-5604(9)	145(9)
C(4B)	1386(10)	-7434(6)	-8455(6)	65(4)
C(5A)	-1532(20)	-7605(9)	-6038(8)	129(8)
C(5B)	816(9)	-6923(5)	-8167(5)	-54(4)
C(6A)	-1880(14)	-6964(7)	-6064(6)	101(5)
C(6B)	62(9)	-7209(5)	-7769(6)	64(4)
C(7A)	-336(22)	-8844(12)	-6867(20)	183(12)
C(7B)	1724(13)	-5702(6)	-9007(6)	72(4)
C(8A)	-921(23)	-8748(10)	-7367(12)	190(12)
C(8B)	671(11)	-5550(6)	-9219(6)	81(5)
C(9A)	476(21)	-9316(10)	-6660(15)	231(15)
C(9B)	2556(10)	-5286(6)	-9215(5)	71(4)
C(10A)	-1945(38)	-8088(19)	-4580(12)	230(22)
C(10B)	2660(10)	-7960(7)	-7955(8)	89(5)
C(11A)	-3018(30)	-8257(12)	-4364(11)	230(13)
C(11B)	2994(12)	-8547(7)	-8309(8)	122(6)
C(12A)	-956(55)	-7761(22)	-4225(10)	731(63)
C(12B)	2971(16)	-7928(8)	-7355(7)	137(7)
C(13A)	-577(11)	-6518(6)	-6629(7)	78(5)
C(13B)	-391(10)	-6234(6)	-7215(6)	66(4)
Pd(2)	-3197(1)	-5941(1)	-7869(1)	58(1)
Cl(1C)	-2685(3)	-5401(2)	-7085(2)	78(1)
Cl(1D)	-1818(3)	-5703(1)	-8394(2)	73(1)
O(1C)	-5517(8)	-4721(4)	-8453(4)	73(3)
O(1D)	-5962(7)	-7312(4)	-9647(4)	77(3)
O(2C)	-4993(6)	-3968(4)	-7880(5)	75(3)
O(2D)	-4943(8)	-7314(5)	-10417(4)	82(3)
O(3C)	-6958(8)	-4284(4)	-6916(4)	90(3)
O(3D)	-5264(8)	-5737(5)	-10675(4)	79(3)
O(4C)	-6052(10)	-4970(5)	-6438(5)	103(4)

O 4D)	-4090(8)	-5465(6)	-10068(4)	100(4)
O(5C)	-6018(6)	-5233(4)	-7682(4)	66(2)
O(5D)	-5408(7)	-6332(4)	-9498(3)	58(2)
N(1C)	-4459(7)	-6231(4)	-7474(4)	56(3)
N(1D)	-3688(7)	-6443(4)	-8542(4)	49(3)
C(1C)	-6189(11)	-4706(6)	-8019(6)	59(4)
C(1D)	-5960(11)	-6703(7)	-9859(5)	65(4)
C(2C)	-5958(10)	-4122(6)	-7712(5)	62(4)
C(2D)	-5474(12)	-6755(6)	-10456(6)	76(5)
C(3C)	-5917(11)	-4143(7)	-7080(8)	88(5)
C(3D)	-4719(11)	-6283(6)	-10595(6)	66(4)
C(4C)	-5389(12)	-4739(7)	-6827(6)	79(5)
C(4D)	-4014(11)	-6127(7)	-10091(6)	73(4)
C(5C)	-5169(10)	-5192(7)	-7306(6)	74(4)
C(5D)	-4350(9)	-6389(6)	-9540(6)	65(4)
C(6C)	-4979(9)	-5834(5)	-7051(6)	64(4)
C(6D)	-3922(9)	-6027(6)	-9018(5)	60(4)
C(7C)	-4896(12)	-4167(7)	-8450(7)	81(5)
C(7D)	-5532(13)	-7732(8)	-10067(7)	98(6)
C(8C)	-3830(11)	-4354(7)	-8570(7)	99(6)
C(8D)	-4795(13)	-8126(6)	-9722(7)	94(5)
C(9C)	-5377(16)	-3711(7)	-8851(7)	125(7)
C(9D)	-6343(12)	-8084(7)	-10386(7)	100(6)
C(10C)	-7004(13)	-4661(8)	-6425(8)	91(5)
C(10D)	-4641(12)	-5252(7)	-10525(7)	78(5)
C(11C)	-6981(16)	-4297(8)	-5877(7)	133(7)
C(11D)	-3957(13)	-5085(7)	-11035(7)	117(6)
C(12C)	-7799(15)	-5117(9)	-6499(9)	135(7)
C(12D)	-5197(13)	-4711(7)	-10312(6)	90(5)
C(13C)	-5141(9)	-6453(5)	-7946(6)	61(4)
C(13D)	-4522(9)	-6855(6)	-8323(6)	63(4)

Table 3. Bond lengths [Å] and angles [°].

Pd(l)-N(lB)	2.070(9)	Pd(l)-N(lA)	2.103(10)
Pd(l)-Cl(lA)	2.318(3)	Pd(l)-Cl(lB)	2.317(4)
O(1A)-C(lA)	1.41(5)	O(lA)-C(7A)	1.61(3)
O(lB)-C(7B)	1.459(14)	O(lB)-C(lB)	1.429(14)
O(2A)-C(2A)	1.48(3)	O(2A)-C(7A)	1.62(3)
O(2B)-C(2B)	1.443(13)	O(2B)-C(7B)	1.429(13)
O(3A)-C(10A)	1.29(5)	O(3A)-C(3A)	1.58(4)
O(3B)-C(3B)	1.416(13)	O(3B)-C(10B)	1.456(15)
O(4A)-C(4A)	1.48(2)	O(4A)-C(10A)	1.59(4)
O(4B)-C(4B)	1.427(14)	O(4B)-C(10B)	1.430(15)
O(5A)-C(5A)	1.44(2)	O(5A)-C(lA)	1.29(4)
O(5B)-C(lB)	1.395(14)	O(5B)-C(5B)	1.450(12)
N(lA)-C(6A)	1.45(2)	N(lA)-C(13A)	1.49(2)
N(lB)-C(6B)	1.535(14)	N(lB)-C(13B)	1.57(2)
C(lA)-C(2A)	1.69(6)	C(lB)-C(2B)	1.54(2)
C(2A)-C(3A)	1.47(4)	C(2B)-C(3B)	1.54(2)
C(3A)-C(4A)	1.60(4)	C(3B)-C(4B)	1.56(2)
C(4A)-C(5A)	1.63(3)	C(4B)-C(5B)	1.53(2)
C(5A)-C(6A)	1.50(2)	C(5B)-C(6B)	1.53(2)
C(7A)-C(8A)	1.45(4)	C(7A)-C(9A)	1.60(4)
C(7B)-C(9B)	1.54(2)	C(7B)-C(8B)	1.56(2)

C(10A)-C(11A)	1.59(5)	C(10A)-C(12A)	1.75(6)
C(10B)-C(12B)	1.49(2)	C(10B)-C(11B)	1.61(2)
C(13A)-C(13B)	1.55(2)	Pd(2)-N(1C)	2.061(9)
Pd(2)-N(1D)	2.059(9)	Pd(2)-Cl(lD)	2.316(4)
Pd(2)-Cl(1C)	2.317(4)	O(lC)-C(1C)	1.377(14)
O(lC)-C(7C)	1.49(2)	O(lD)-C(1D)	1.44(2)
O(lD)-C(7D)	1.48(2)	O(2C)-C(7C)	1.43(2)
O(2C)-C(2C)	1.416(14)	O(2D)-C(7D)	1.48(2)
O(2D)-C(2D)	1.438(15)	O(3C)-C(10C)	1.43(2)
O(3C)-C(3C)	1.50(2)	O(3D)-C(10D)	1.42(2)
O(3D)-C(3D)	1.4134(15)	O(4C)-C(4C)	1.39(2)
O(4C)-C(10C)	1.47(2)	O(4D)-C(10D)	1.40(2)
O(4D)-C(4D)	1.47(2)	O(5C)-C(1C)	1.435(13)
O(5C)-C(5C)	1.464(14)	O(5D)-C(lD)	1.404(15)
O(5D)-C(5D)	1.452(13)	N(1C)-C(13C)	1.536(15)
N(1C)-C(6C)	1.510(14)	N(1D)-C(6D)	1.491(14)
N(lD)-C(13D)	1.547(14)	C(lC)-C(2C)	1.52(2)
C(lD)-C(2D)	1.57(2)	C(2C)-C(3C)	1.50(2)
C(2D)-C(3D)	1.50(2)	C(3C)-C(4C)	1.62(2)
C(3D)-C(4D)	1.57(2)	C(4C)-C(5C)	1.54(2)
C(4D)-C(5D)	1.50(2)	C(5C)-C(6C)	1.57(2)
C(5D)-C(6D)	1.59(2)	C(7C)-C(8C)	1.54(2)
C(7C)-C(9C)	1.53(2)	C(7D)-C(9D)	1.55(2)
C(7D)-C(8D)	1.56(2)	C(10C)-C(12C)	1.49(2)
C(10C)-C(llC)	1.53(2)	C(10D)-C(12D)	1.50(2)
C(10D)-C(11D)	1.57(2)	C(13C)-C(13D)	1.52(2)

N(lB)-Pd(l)-N(lA)	85.1(4)	N(1B)-Pd(l)-Cl(lA)	176.3(3)
N(lA)-Pd(l)-Cl(lA)	92.6(3)	N(lB)-Pd(l)-Cl(1B)	89.2(3)
N(lA)-Pd(l)-Cl(lB)	174.3(3)	Cl(lA)-Pd(l)-Cl(lB)	93.10(13)
C(1A)-O(lA)-C(7A)	129(3)	C(7B)-O(lB)-C(lB)	112.5(9)
C(2A)-O(2A)-C(7A)	119(3)	C(2B)-O(2B)-C(7B)	107.0(10)
C(10A)-O(3A)-C(3A)	119(4)	C(3B)-O(3B)-C(10B)	111.6(10)
C(4A)-O(4A)-C(10A)	107.2(19)	C(4B)-O(4B)-C(10B)	114.5(10)
C(5A)-O(5A)-C(lA)	116(3)	C(lB)-O(5B)-C(5B)	115.2(9)
C(6A)-N(1A)-C(13A)	112.0(13)	C(6A)-N(lA)-Pd(l)	118.4(9)
C(13A)-N(lA)-Pd(l)	106.0(8)	C(6B)-N(lB)-C(13B)	113.9(9)
C(6B)-N(lB)-Pd(l)	110.7(7)	C(13B)-N(lB)-Pd(l)	106.8(7)
O(1A)-C(lA)-O(5A)	112(5)	O(lA)-C(1A)-C(2A)	97(3)
O(5A)-C(lA)-C(2A)	118(4)	O(5B)-C(lB)-O(1B)	112.1(10)
O(5B)-C(lB)-C(2B)	115.0(10)	O(1B)-C(lB)-C(2B)	101.7(10)
C(3A)-C(2A)-O(2A)	101(2)	C(3A)-C(2A)-C(lA)	109(3)
O(2A)-C(2A)-C(1A)	99(3)	O(2B)-C(2B)-C(lB)	103.2(9)
O(2B)-C(2B)-C(3B)	105.3(10)	C(lB)-C(2B)-C(3B)	113.0(11)
C(2A)-C(3A)-O(3A)	106(4)	C(2A)-C(3A)-C(4A)	127(3)
O(3A)-C(3A)-C(4A)	95(3)	O(3B)-C(3B)-C(2B)	105.2(10)
O(3B)-C(3B)-C(4B)	103.3(10)	C(2B)-C(3B)-C(4B)	114.7(11)
O(4A)-C(4A)-C(5A)	107.0(16)	O(4A)-C(4A)-C(3A)	107.6(19)
C(5A)-C(4A)-C(3A)	103(2)	O(4B)-C(4B)-C(5B)	110.5(11)
O(4B)-C(4B)-C(3B)	102.6(10)	C(5B)-C(4B)-C(3B)	112.4(11)
O(5A)-C(5A)-C(6A)	109.3(18)	O(5A)-C(5A)-C(4A)	113.7(18)
C(6A)-C(5A)-C(4A)	108.7(19)	O(5B)-C(5B)-C(6B)	108.9(10)
O(5B)-C(5B)-C(4B)	109.0(10)	C(6B)-C(5B)-C(4B)	108.0(10)
N(lA)-C(6A)-C(5A)	113.1(14)	C(5B)-C(6B)-N(1B)	106.3(9)

C(8A)-C(7A)-O(2A)	109(3)	C(8A)-C(7A)-C(9A)	137(3)
O(2A)-C(7A)-C(9A)	95(3)	C(8A)-C(7A)-O(1A)	120(2)
O(2A)-C(7A)-O(1A)	85(2)	C(9A)-C(7A)-O(1A)	96(2)
O(2B)-C(7B)-O(1B)	102.3(9)	O(2B)-C(7B)-C(9B)	111.2(12)
O(1B)-C(7B)-C(9B)	108.8(12)	O(2B)-C(7B)-C(8B)	109.1(12)
O(1B)-C(7B)-C(8B)	108.1(12)	C(9B)-C(7B)-C(8B)	116.5(11)
O(3A)-C(10A)-C(11A)	126(3)	O(3A)-C(10A)-C(12A)	91(5)
C(11A)-C(10A)-C(12A)	131(3)	O(3A)-C(10A)-O(4A)	99(2)
C(11A)-C(10A)-O(4A)	98(3)	C(12A)-C(10A)-O(4A)	107(2)
O(3B)-C(10B)-C(12B)	108.3(13)	O(3B)-C(10B)-O(4B)	102.0(10)
C(12B)-C(10B)-O(4B)	115.9(16)	O(3B)-C(10B)-C(11B)	106.4(13)
C(12B)-C(10B)-C(11B)	117.0(13)	O(4B)-C(10B)-C(11B)	105.9(13)
N(1A)-C(13A)-C(13B)	107.8(12)	C(13A)-C(13B)-N(1B)	105.7(10)
N(1C)-Pd(2)-N(1D)	84.9(4)	N(1C)-Pd(2)-Cl(1D)	173.1(3)
N(1D)-Pd(2)-Cl(1D)	88.3(3)	N(1C)-Pd(2)-Cl(1C)	92.8(3)
N(1D)-Pd(2)-Cl(1C)	177.5(3)	Cl(1D)-Pd(2)-Cl(1C)	93.94(13)
C(1C)-O(1C)-C(7C)	110.8(10)	C(1D)-O(1D)-C(7D)	110.7(11)
C(7C)-O(2C)-C(2C)	106.2(10)	C(7D)-O(2D)-C(2D)	107.6(11)
C(10C)-O(3C)-C(3C)	111.7(12)	C(10D)-O(3D)-C(3D)	107.2(11)
C(4C)-O(4C)-C(10C)	114.6(12)	C(10D)-O(4D)-C(4D)	110.2(12)
C(1C)-O(5C)-C(5C)	114.6(10)	C(1D)-O(5D)-C(5D)	116.1(10)
C(13C)-N(1C)-C(6C)	112.6(9)	C(13C)-N(1C)-Pd(2)	106.0(7)
C(6C)-N(1C)-Pd(2)	120.8(7)	C(6D)-N(1D)-C(13D)	117.4(9)
C(6D)-N(1D)-Pd(2)	108.7(7)	C(13D)-N(1D)-Pd(2)	107.3(7)
O(1C)-C(1C)-O(5C)	106.7(10)	O(1C)-C(1C)-C(2C)	103.9(11)
O(5C)-C(1C)-C(2C)	113.2(10)	O(5D)-C(1D)-O(1D)	109.7(10)
O(5D)-C(1D)-C(2D)	111.5(12)	O(1D)-C(1D)-C(2D)	104.3(10)
O(2C)-C(2C)-C(3C)	104.8(12)	O(2C)-C(2C)-C(1C)	105.2(10)
C(3C)-C(2C)-C(1C)	117.3(12)	O(2D)-C(2D)-C(3D)	105.6(12)
O(2D)-C(2D)-C(1D)	102.6(11)	C(3D)-C(2D)-C(1D)	115.9(12)
C(2C)-C(3C)-O(3C)	103.3(12)	C(2C)-C(3C)-C(4C)	114.3(12)
O(3C)-C(3C)-C(4C)	99.0(12)	O(3D)-C(3D)-C(2D)	105.1(12)
O(3D)-C(3D)-C(4D)	103.4(11)	C(2D)-C(3D)-C(4D)	113.9(12)
O(4C)-C(4C)-C(5C)	112.1(13)	O(4C)-C(4C)-C(3C)	104.8(12)
C(5C)-C(4C)-C(3C)	110.2(12)	O(4D)-C(4D)-C(5D)	109.4(12)
O(4D)-C(4D)-C(3D)	101.8(12)	C(5D)-C(4D)-C(3D)	112.9(12)
O(5C)-C(5C)-C(6C)	107.9(11)	O(5C)-C(5C)-C(4C)	109.5(11)
C(6C)-C(5C)-C(4C)	109.8(12)	O(5D)-C(5D)-C(4D)	109.2(11)
O(5D)-C(5D)-C(6D)	105.6(10)	C(4D)-C(5D)-C(6D)	111.7(11)
N(1C)-C(6C)-C(5C)	110.5(10)	N(1D)-C(6D)-C(5D)	110.8(10)
O(2C)-C(7C)-C(8C)	110.2(14)	O(2C)-C(7C)-O(1C)	101.8(11)
C(8C)-C(7C)-O(1C)	108.3(11)	O(2C)-C(7C)-C(9C)	110.1(12)
C(8C)-C(7C)-C(9C)	117.8(15)	O(1C)-C(7C)-C(9C)	107.3(13)
O(2D)-C(7D)-O(1D)	101.4(12)	O(2D)-C(7D)-C(9D)	115.4(13)
O(1D)-C(7D)-C(9D)	111.2(13)	O(2D)-C(7D)-C(8D)	107.0(13)
O(1D)-C(7D)-C(8D)	104.7(12)	C(9D)-C(7D)-C(8D)	115.7(15)
O(3C)-C(10C)-O(4C)	102.6(13)	O(3C)-C(10C)-C(12C)	109.3(15)
O(4C)-C(10C)-C(12C)	108.9(13)	O(3C)-C(10C)-C(11C)	112.5(14)
O(4C)-C(10C)-C(11C)	104.1(14)	C(12C)-C(10C)-C(11C)	118.1(17)
O(3D)-C(10D)-O(4D)	105.2(11)	O(3D)-C(10D)-C(12D)	112.7(13)
O(4D)-C(10D)-C(12D)	106.3(14)	O(3D)-C(10D)-C(11D)	109.9(13)
O(4D)-C(10D)-C(11D)	110.9(13)	C(12D)-C(10D)-C(11D)	111.7(13)
N(1C)-C(13C)-C(13D)	106.2(10)	C(13C)-C(13D)-N(1D)	105.2(9)

Table 5. Anisotropic displacement parameters [Å^2 x 10^3]. The anisotropic displacement factor exponent takes the form: $-2\pi^2\left[(ha^*)^2 U_{11} + \ldots + 2hka^*b^*U_{12}\right]$

Pd(l)	58(l)	49(l)	75(l)	2(l)	4(l)	-5(l)
Cl(lA)	66(2)	62(2)	98(3)	18(2)	14(2)	-12(2)
Cl(lB)	65(3)	62(2)	88(3)	-8(2)	3(2)	3(2)
O(lA)	116(13)	94(14)	454(36)	36(17)	27(18)	-21(10)
O(1B)	89(8)	57(6)	79(7)	-11(5)	-4(6)	8(6)
O(2A)	278(24)	84(11)	210(19)	21(12)	-95(20)	-22(13)
O(2B)	68(6)	56(6)	67(6)	-11(4)	5(6)	0(6)
O(3A)	346(39)	160(19)	243(30)	-12(18)	47(26)	67(20)
O(3B)	56(6)	72(6)	80(6)	-9(5)	-21(6)	2(6)
O(4A)	409(28)	97(10)	123(12)	10(10)	41(15)	-24(13)
O(4B)	63(7)	66(6)	136(9)	20(6)	4(6)	8(5)
O(5A)	192(19)	114(14)	272(21)	48(14)	-102(17)	-69(14)
O(5B)	51(6)	67(6)	63(6)	-5(5)	-1(5)	-7(4)
N(lA)	96(11)	70(7)	44(7)	1(6)	8(7)	-19(7)
N(lB)	50(7)	54(7)	78(8)	8(6)	21(6)	0(5)
C(lA)	406(73)	190(39)	530(88)	-186(51)	-72(60)	116(45)
C(lB)	50(9)	58(9)	66(10)	-17(8)	9(8)	-2(8)
C(2A)	109(17)	62(15)	292(35)	-3(17)	-107(20)	-5(12)
C(2B)	48(8)	49(8)	65(9)	10(7)	-7(8)	17(7)
C(3A)	444(60)	105(22)	183(32)	20(20)	-117(40)	18(32)
C(3B)	48(9)	50(9)	84(10)	8(7)	-13(8)	7(7)
C(4A)	243(27)	83(14)	109(16)	-1(13)	29(17)	-4(16)
C(4B)	60(10)	61(10)	74(11)	11(8)	-6(8)	1(8)
C(5A)	176(24)	91(15)	118(16)	27(12)	-13(16)	-47(15)
C(5B)	42(8)	53(9)	67(9)	-27(7)	-2(7)	-13(7)
C(6A)	129(15)	87(12)	88(12)	17(9)	12(13)	4(12)
C(6B)	50(8)	41(8)	100(11)	-6(7)	16(8)	6(7)
C(7A)	139(25)	88(20)	321(47)	2(25)	18(27)	-13(17)
C(7B)	119(14)	49(9)	48(9)	-12(7)	9(10)	9(10)
C(8A)	252(31)	137(20)	180(25)	23(17)	-98(23)	11(19)
C(8B)	72(12)	57(10)	114(13)	-1(9)	-27(10)	31(8)
C(9A)	207(28)	91(17)	396(42)	57(23)	55(28)	48(19)
C(9B)	82(11)	72(10)	59(10)	2(8)	16(8)	-28(9)
C(10A)	323(55)	262(44)	104(21)	58(24)	-8(29)	-164(44)
C(10B)	48(10)	58(10)	159(17)	42(11)	-17(10)	4(8)
C(11A)	328(39)	160(24)	201(28)	20(19)	63(31)	-20(29)
C(11B)	65(11)	69(11)	232(20)	-9(11)	13(14)	17(10)
C(12A)	1558(166)	553(70)	81(20)	11(29)	-228(46)	-659(94)
C(12B)	197(20)	149(16)	65(10)	24(11)	-55(14)	-18(17)
C(13A)	62(11)	59(10)	114(14)	-17(9)	11(10)	-12(8)
C(13B)	68(10)	50(8)	80(12)	-11(8)	-3(9)	-6(7)
Pd(2)	48(l)	49(l)	77(l)	-1(1)	-5(l)	-4(l)
Cl(lC)	72(2)	68(2)	95(3)	-21(2)	-13(2)	-2(2)
Cl(1D)	58(2)	63(2)	99(3)	12(2)	-6(2)	-7(2)
O(lC)	90(8)	61(7)	69(7)	-7(5)	-11(6)	-2(6)
O(lD)	78(7)	70(7)	82(7)	6(6)	37(6)	4(6)
O(2C)	71(7)	54(6)	100(8)	-20(6)	6(6)	-2(5)
O(2D)	108(9)	91(8)	48(6)	-8(5)	9(6)	18(7)
O(3C)	84(8)	79(7)	106(8)	-16(6)	19(7)	5(6)
O(3D)	88(8)	82(8)	67(7)	12(6)	4(6)	16(7)
O(4C)	138(11)	100(g)	72(8)	23(6)	39(8)	27(8)

O(4D)	90(8)	123(11)	86(8)	31(8)	-33(7)	-36(7)
O(5C)	57(6)	56(6)	84(7)	-18(5)	-12(6)	-2(5)
O(5D)	71(7)	60(6)	44(6)	-15(4)	13(5)	-7(5)
N(lC)	44(6)	48(6)	77(8)	-13(6)	13(6)	4(5)
N(lD)	58(7)	55(7)	35(6)	4(5)	-4(5)	-6(5)
C(lc)	94(11)	39(8)	43(9)	5(7)	11(8)	13(7)
C(lD)	71(11)	82(12)	41(9)	-13(8)	4(8)	14(9)
C(2C)	76(10)	70(10)	41(10)	-12(8)	18(8)	-15(8)
C(2D)	98(13)	49(9)	81(12)	3(8)	20(10)	40(9)
C(3C)	57(10)	92(12)	115(15)	-12(11)	1(10)	26(9)
C(3D)	84(12)	47(9)	67(11)	14(8)	15(9)	3(9)
C(4C)	108(13)	70(10)	58(10)	-16(8)	9(10)	27(10)
C(4D)	63(10)	90(13)	65(11)	-2(9)	16(9)	-9(9)
C(5C)	51(9)	98(12)	74(11)	-20(9)	-2(9)	4(8)
C(5D)	26(8)	104(12)	66(11)	9(9)	6(8)	4(8)
C(6C)	67(9)	47(8)	77(10)	9(8)	5(8)	11(7)
C(6D)	62(9)	51(9)	67(10)	10(8)	-6(8)	5(7)
C(7C)	108(14)	50(10)	85(13)	-14(9)	20(11)	-11(10)
C(7D)	101(15)	118(16)	76(12)	9(12)	38(11)	17(13)
C(8C)	65(11)	82(12)	148(16)	-30(11)	23(11)	3(9)
C(8D)	113(14)	62(11)	108(13)	1(9)	-13(11)	23(10)
C(9C)	214(21)	78(12)	84(13)	36(10)	5(14)	34(13)
C(9D)	123(14)	69(11)	107(13)	-27(9)	-45(11)	-22(10)
C(10C)	61(12)	81(12)	130(16)	3(11)	8(12)	20(11)
C(10D)	78(12)	72(12)	82(12)	15(10)	-6(10)	-10(10)
C(11C)	143(16)	166(17)	90(12)	-82(12)	33(13)	2(15)
C(11D)	112(14)	116(14)	124(15)	72(11)	52(13)	7(11)
C(12C)	108(17)	135(16)	162(19)	-4(14)	32(14)	-25(14)
C(12D)	135(15)	66(10)	71(11)	-5(8)	25(10)	42(10)
C(13C)	56(9)	57(8)	69(10)	-14(8)	4(8)	-25(7)
C(13D)	52(9)	50(8)	86(11)	-1(7)	29(8)	-21(7)

Project 2

1,2-*O*-Isopropylidene-α-D-xylofuranose (10) to 5-deoxy-5-tosyl-1,2-*O*-isopropylidene-α-D-xylofuranose (11).

1,2-*O*-isopropylidene-α-D-xylofuranose (**10**) (2.8 g, FW=190.2, 15mmol) was dissolved in 15 mL of pyridine and cooled to 0 °C. A solution of p-toluenesulfonyl chloride (3.09g, 1.1 eq) in 10 mL $CHCl_3$ was added dropwise and the solution was stirred overnight, at which time TLC using ethyl acetate as eluent showed complete reaction. Water (5 mL) was then added and stirred for 30 min. The mixture was then extracted with $CHCl_3$ (3x15 mL), followed by washings with 5% sulfuric acid (2x25 mL) and a final washing with water (20 mL). The organic layer was dried over $MgSO_4$, and evaporated to yield the product tosylate (**11**) in 68% (3.5 g).

5-Deoxy-5-tosyl-1,2-*O*-isopropylidene-α-D-xylofuranose (11) to 5-azido-5-deoxy-1,2-*O*-isopropylidene-α-D-xylofuranose (12).

5-Deoxy-5-tosyl-1,2-*O*-isopropylidene-α-D-xylofuranose (4.21g, FW= 344.37, 12.2 mmol) was dissolved in 150 mL DMF, to which was added sodium azide (3.18g, 4 eq), urea (100 mg) and water (2 mL). This was heated to reflux and stirred overnight. The reaction mixture was then evaporated under vacuum, and the residue dissolved in $CHCl_3$ (50 mL) and added to 50 mL water. This was extracted with $CHCl_3$ (3x25 mL), followed by drying over $MgSO_4$ and evaporation of solvent. The resultant syrup was extracted into hot hexane (6x25 mL) and the combined extracts cooled in a freezer overnight. This was then filtered to yield product azide (**12**) as white crystals with a yield of 60% (1.57 g).

5-Azido-5-deoxy-1,2-*O*-isopropylidene-α-D-xylofuranose (12) to 5-deoxy-1,2-*O*-isopropylidene-5-*C*-(4,5-diphenyl-1,2,3-triazol-1-yl)-α-D-xylofuranose (16).[25]

The azide (**12**, 337 mg, 1.52 mmol) and diphenylacetylene (1.1 g, 6.1 mmol) were refluxed in *o*-xylene (13 mL) for 72 h after which time TLC (hexane-EtOAc 4:1) showed complete reaction. The solvent was evaporated and the residue purified by flash chromatography to give triazole **16** (289 mg, 48%) as a colorless solid, mp 227-229 °C: $[\alpha]_D$ –72.7° (*c*, 2.1, CH_2Cl_2). Exact mass calculated for $C_{22}H_{23}N_3O_4$: 393.1689. Found: 393.1673.

^{1}H NMR (δ): 7.27-7.55 (m, 10H, phenyl); 5.95 (d, 1H, *J* = 3.5 Hz, H-1); 4.64 (d, 1H, *J* = 3.6 Hz, H-2); 4.57 (m, 1H, H-5); 4.36 (m, 2H, H-4, H-5'); 4.26 (s, 1H, OH); 3.77 (d, 1H, *J* = 4.0 Hz, H-3).

^{13}C NMR (δ): 27.3, 28.1, 46.3, 75.7, 80.4, 86.0, 100.8, 106.3, 127.8, 128.0, 129.0, 129.6, 130.6, 130.9, 131.2, 135.6.

5-Azido-5-deoxy-1,2-*O*-isopropylidene-α-D-xylofuranose (12) to 5-deoxy-1,2-*O*-isopropylidene-5-*C*-(1,2,3-triazol-1-yl)-α-D-xylofuranose (17).[25]

Azide **12** (300 mg, 1.35 mmol) and phenyl vinyl sulfoxide (0.89 mL, 5.42 mmol) were refluxed in *o*-xylene (13 mL) for 30 h after which time TLC (hexane-EtOAc 4:1) showed reaction to be complete. The solvent was evaporated and the residue resolved by flash chromatography to give the parent triazole (**17,** 221 mg) as a colorless syrup in 68%. This material was contaminated with a byproduct, the signals for which showed at 5.9, 6.2 and 7.2-8.0 ppm in the ^{1}H NMR.

^{1}H and ^{13}C NMR data for pure triazole formed on the polymer support are given below.

Synthesis of Polymer-supported Azide (20).[25]

Polyethylene glycol monomethyl ether (MW ~5000, 25 g, 5 mmol) was dissolved in 250 mL dry CH_2Cl_2 and 50 mL pyridine. To this, succinic anhydride (10 g, 100 mmol) and 4-DMAP (1 g) were added. The mixture was stirred at RT for 24 h then evaporated to ~ half volume and the remainder cooled in an ice-water bath. Ice-cold ether (1200 mL) was then added with stirring and the resultant white solid was collected by vacuum filtration and subsequently recrystallized from EtOAc-hexane (~25 g, ~100% yield). ^{1}H NMR (with suppression of polymer methylene signals) showed >95% loading of the succinate linker.

This material (5.14 g, ~1.1 mmol) was dissolved in 25 mL CH_2Cl_2 and 25 mL MeCN. To this solution was added azide (**12**) (0.44 g, 2 mmol), DMAP (0.24 g) and a solution of dicyclohexylcarbodiimide (1.5 mL, 1 M in CH_2Cl_2). The mixture was stirred for 24 h at rt after which time the precipitate was filtered and washed with CH_2Cl_2 (~5 mL). The mixture was evaporated back to ~ 50 mL and then cooled in ice-water while ice-cold diethyl ether (250 mL) was added with vigorous stirring. The precipitate (**20**) was filtered and recrystallized from absolute ethanol (4.90 g, ~98%, mp 50-52 °C)

^{1}H NMR (δ): 5.95 (d, 1H, J = 3.7 Hz, H-1); 5.22 (d, 1H, J = 3.1 Hz, H-3); 4.55 (d, 1H, J = 3.7 Hz, H-2); 4.40 (m, 1H, H-4); 4.25 (m, 2H, H-5,H-5'); 3.81 (m, 2H, CH_2O, polymer); 3.38 (s, 3H, OCH_3, polymer); 2.68 (m, 4H, CH_2CH_2, linker); 1.54 (s, 3H, CH_3), 1.33 (s, 3H, CH_3).

Cycloaddition of polymer-bound azide 20 with propargyl alcohol.[25]

A solution of azide **20** (2 g, 0.4 mmol) and propargyl alcohol (10 eq) were refluxed in 30 mL toluene for 48 h. The mixture was cooled in ice water then ice-cold ether (500 mL) was added with vigorous stirring to induce precipitation. The solid was filtered and then recrystallized from absolute ethanol to afford the polymer-bound triazole **21** with a cycloaddition efficiency of >95% and a polymer recovery of 94% (1.88 g).

^{1}H NMR (δ) (for the mixture of regioisomers): 7.69, 7.59 (2s, 1H total, triazole) 5.91 5.92 (2d, 1H total, J = 3.5 Hz, H-1); 5.22, 5.31 (2d, 1H total, J = 2.8 Hz, H-3) 4.2-4.5 (m, 4H total, H-2, 4, 5, 5'); 4.20 (m, CH_2O, polymer); 3.35 (s, 3H, OCH_3, polymer); 2.65 (m, 4H, CH_2CH_2); 1.43s, 1.41s, 1.27s, 1.26s (6H total, 2 CH_3).

Cycloaddition of polymer-bound azide 20 with ethyl propiolate.[25]

A solution of azide **20** (2 g, 0.4 mmol) and ethyl propiolate (10 eq) were refluxed in 30 mL toluene for 48 h. The mixture was cooled in ice water then ice-cold ether (500 mL) was added with vigorous stirring to induce precipitation. The solid was filtered then recrystallized from absolute ethanol to afford the polymer-bound triazole **22** with a cycloaddition efficiency of >95% and a polymer recovery of 93% (1.86 g).

^{1}H NMR (δ) (for the mixture of regioisomers): 8.24, 8.10 (2s, 1H total, triazole) 5.91, 5.94 (2d, 1H total, J = 3.7 Hz, H-1); 5.29, 5.25 (2d, 1H total, J = 2.9, 3.1 Hz, H-3) 4.2-4.5 (m, 4H total, H-2, 4, 5, 5'); 4.20 (m, CH_2O, polymer); 3.38 (s, 3H, OCH_3, polymer); 2.65 (m, 4H, CH_2CH_2); 1.42s, 1.25s (6H total, 2 CH_3).

Cycloaddition of polymer-bound azide 20 with phenyl vinyl sulfoxide.[25]

A solution of azide **20** (2 g, 0.4 mmol) and phenyl vinyl sulfoxide (10 eq) were refluxed in 30 mL *o*-xylene for 48 h. The mixture was cooled in ice water then ice-cold ether (500 mL) was added with vigorous stirring to induce precipitation. The solid was filtered then recrystallized from absolute ethanol to afford the polymer-bound triazole **23** with a cycloaddition efficiency of >95% and a polymer recovery of 97% (1.94 g).

^{1}H NMR (δ) (for the mixture of regioisomers): 7.71, 7.68 (2s, 1H total, triazole) 5.94 (d, 1H total, J = 3.7 Hz, H-1); 5.25 (d, 1H total, J = 2.6, H-3); 4.70 (dd, 1H, J = 4.0, 14.1 Hz, H-5); 4.61 (m, H-4); 4.55 (m, H-5'); 4.54 (d, 1H, J = 3.3 Hz); 4.20 (m, CH_2O, polymer); 3.35 (s, 3H, OCH_3, polymer); 2.65 (m, 4H, CH_2CH_2); 1.43s, 1.27s (6H total, 2 CH_3).

Cycloaddition of polymer-bound azide 20 with phenyl acetylene.[25]

A solution of azide **20** (2 g, 0.4 mmol) and phenyl acetylene (10 eq) were refluxed in 30 mL toluene for 48 h. The mixture was cooled in ice water then ice-cold ether (500 mL) was added with vigorous stirring to induce precipitation. The solid was filtered then recrystallized from absolute ethanol to afford the polymer-bound triazole **24** with a cycloaddition efficiency of ≈ 50% and a polymer recovery of 97% (1.94 g).

^{1}H NMR (δ) (for the mixture of regioisomers): 7.95, 7.68 (2s, 0.5 H total, triazole) 5.97 5.92 (2d, 0.5 H total, J = 3.7 Hz, H-1); 5.30, 5.21 (2d, 0.5 H total, J = 2.8 Hz, H-3) 4.2-4.5 (m, 2H total, H-2, 4, 5, 5'); 4.20 (m, CH_2O, polymer); 3.35 (s, 3H,

OCH_3, polymer); 2.65 (m, 4H, CH_2CH_2); 1.43s, 1.41s, 1.27s, 1.26s (3H total, 2 x CH_3).

Attempted cycloaddition of polymer-bound azide 20 with diphenyl acetylene.[25]

A solution of azide **20** (2 g, 0.4 mmol) and diphenyl acetylene (10 eq) were refluxed in 30 mL *o*-xylene for 120 h. The mixture was cooled in ice water then ice-cold ether (500 mL) was added with vigorous stirring to induce precipitation. The solid was filtered then recrystallized from absolute ethanol. ^{1}H NMR showed only signals representing starting material.

Removal of triazoles from the polymer support.[25]

Polymer-supported triazole **23** (2.51 g, ~ 0.47 mmol) was dissolved in ice-cold methanol (60 mL) that had been saturated with ammonia. After stirring overnight at rt, the mixture was concentrated to half volume then cold ether (500 mL) was added with stirring. The precipitated polymer was filtered and the filtrate condensed to a syrup which was purified by chromatography using hexane-ethyl acetate (4:1) as eluent. Triazole **17** was isolated as a colorless syrup (0.11 g, 0.44 mmol, ~94%), $[\alpha]_D$ –1.6° (*c*, 0.92, CH_2Cl_2). Exact mass calculated for $C_{10}H_{16}N_3O_4$ ($M+H^+$): 242.1141. Found: 242.1147.

^{1}H NMR (δ): 7.73 (s, 1H, triazole H); 7.70 (s, 1H, triazole H); 6.00 (d, 1H, J = 3.7, H-1); 4.82 (dd, 1H, J = 6.6, 14.1, H-5); 4.60 (d, 1H, J = 3.5, H-2); 4.56 (m, 1H, H-5'); 4.45 (m, 1H, H-4); 4.23 (s, 1H, H-3); 1.28 (s, 3H, CH_3); 1.24 (s, 3H, CH_3).

^{13}C NMR (δ): 27.4, 30.9, 50.1, 75.5, 80.5, 86.5, 106.2, 113.0, 126.1, 134.7.

The NMR spectra of this material were identical to that for **17** formed above, except with the notable absence of byproduct contaminants.

Likewise, polymer **21**, upon treatment with ammonia, afforded the known triazoles **2** (R^1 = CH_2OH, R^2 = H)[24] in 80% yield after flash chromatography using ethyl acetate as eluent. Polymer **22** afforded the known amides **2** (R^1 = $CONH_2$, R_2 = H)[24] in 85% yield after treatment with ammonia and chromatography using toluene-methanol (3:1) as eluent.

References:

1. Collins, P., Ferrier, R. "Monosaccharides," John Wiley and Sons: Chichester, West Sussex, England; 1995 p. 1-4.
2. Satai, P. "The Chemistry of the Azido Group", John Wiley and Sons: London, England; 1971 p. 59.
3. Satai, P. "The Chemistry of the Azido Group", John Wiley and Sons: London, England; 1971 p. 5.
4. Seyden-Penne, J. "Chiral Auxiliaries and Ligands in Asymmetric Synthesis," John Wiley and Sons New York.
5. Jacobsen, E.N., Zhang, W., Muci, A.R., Ecker, J.R., Deng, L. *J. Amer. Chem. Soc.*,**113**, 7063 (1991)
6. Cotton, F.A., Wilkinson, G., "Advanced Inorganic Chemistry," John Wiley and Sons: New York, 1988.
7. Hambley, T., *Coord. Chem. Rev.*, **166**, 183-194 (1997).
8. Thanks to Dr. Tim Wagner for X-ray crystallography.
9. Wilson, S.R., Czarnik, A.W. "Combinatorial Chemistry," John Wiley and Sons: New York 1997 p. 5.
10. Osborn, H.M.I., Khan, T.H., *Tetrahedron* **55**, 1808 (1999).
11. Yedida, V. and Leznoffm C.C., *Can J. Chem.* **58**, 1144 (1980).
12. Kurth, M.J., Randall, L.A. Chen, C., Melander, C., Miller, R.B., *J. Org. Chem.* **59**, 5862-5864 (1994).
13. Kurth, M.J., Randall, L.A. Chen, C., Jones, D.A., Miller, R.B., *J. Am. Chem. Soc.* **116**, 2661-2662 (1994).

14. Wilson, S.R., Czarnik, A.W. "Combinatorial Chemistry," John Wiley and Sons: New York 1997 p. 1.

15. Weremuth, C.G ed. "The Practice of Medicinal Chemistry," Academic Press: San Diego, CA 1996 p. 123.

16. http://www.5z.com/divinfo/upto_ly.html

17. Wilson, S.R., Czarnik, A.W. "Combinatorial Chemistry," John Wiley and Sons: New York 1997 p. 10.

18. Janda, K.D., Gravert, D.J., *Chem. Rev.* **97,** 491 (1997).

19. Janda, K.D., Gravert, D.J., *Chem. Rev.* **97,** 502 (1997).

20. Janda, K.D., Gravert, D.J., *Chem. Rev.* **97,** 504 (1997).

21. Collins, P., Bauer, D.J., *J. Antimicrob. Chemoth.* **5,** 431 (1979).

22. Ryan, K.J., Acton, A.M., Goodman, L. *J. Am. Chem. Soc.* **84** 3597 (1966).

23. Horowitz, J.P, Chua, Noel, M. *J. Org. Chem.* **29,** 2076 (1964).

24. Norris, P., Horton, D.Levine, B.R., *Heterocycles* **43,** (12) 2643 (1996).

25. Freeze, S., Norris, P., *Heterocycles* **51,** (8) 1999 (to be published).

Appendix

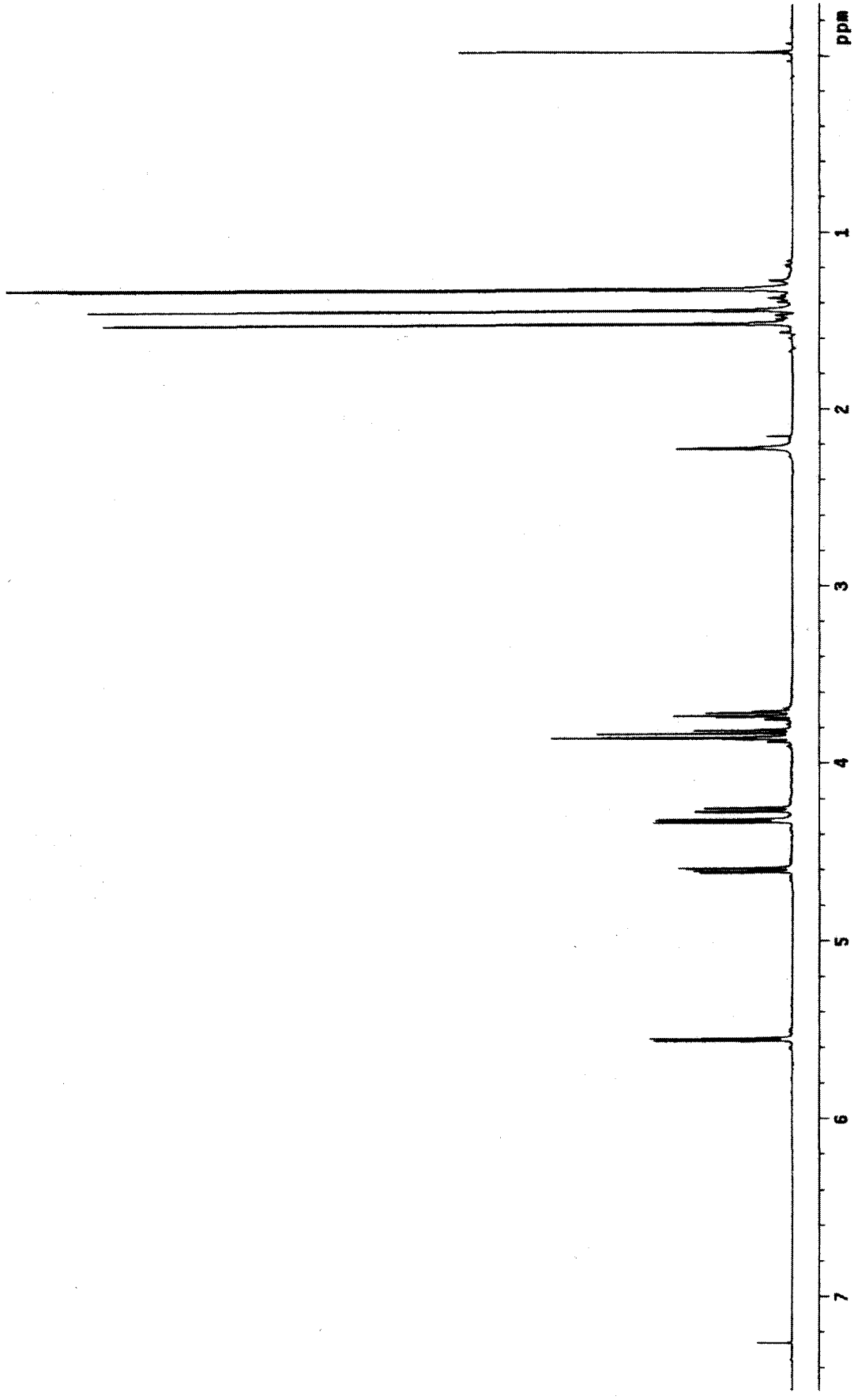

Figure 19. ^{1}H NMR of **1**

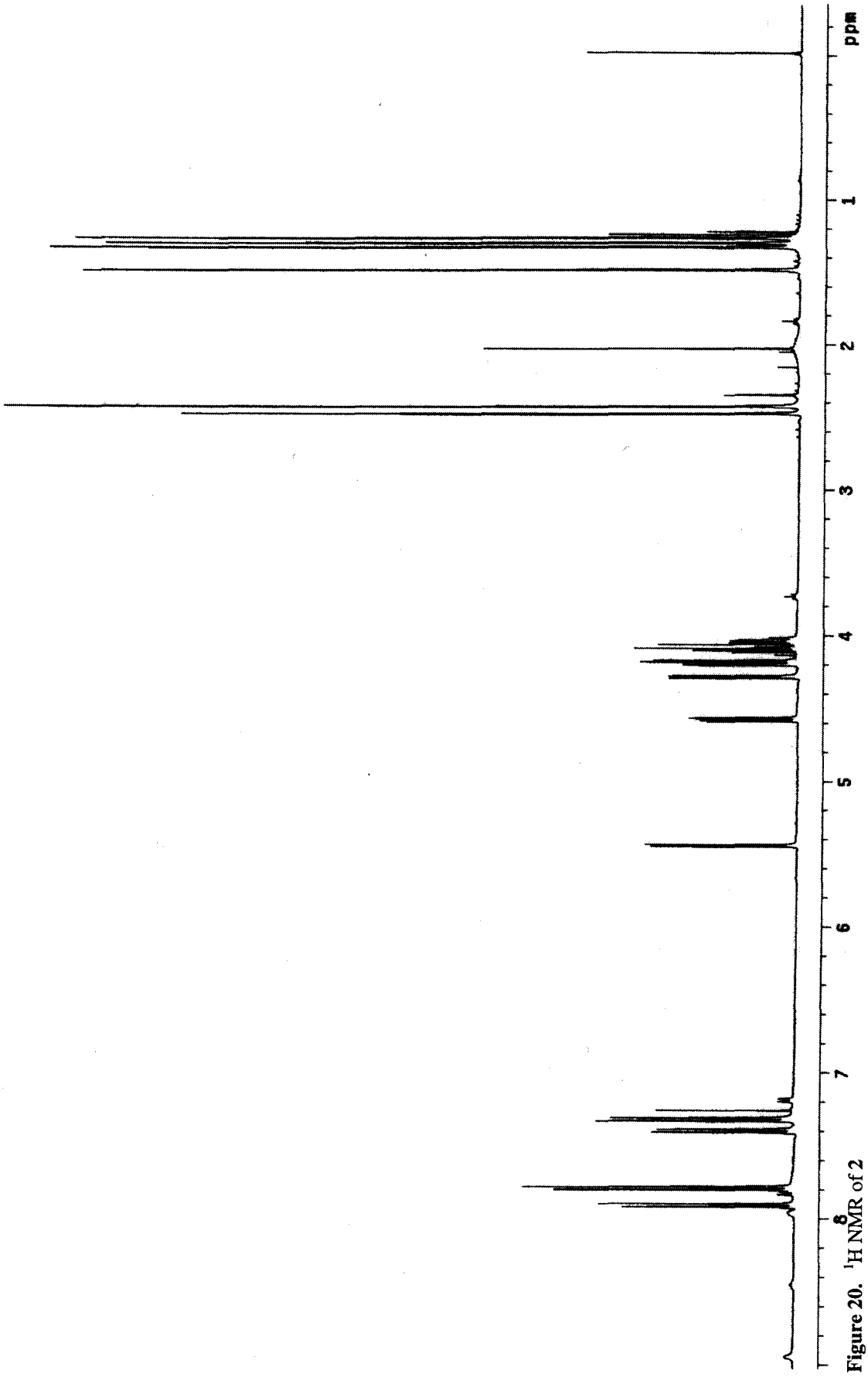

Figure 20. ^{1}H NMR of **2**

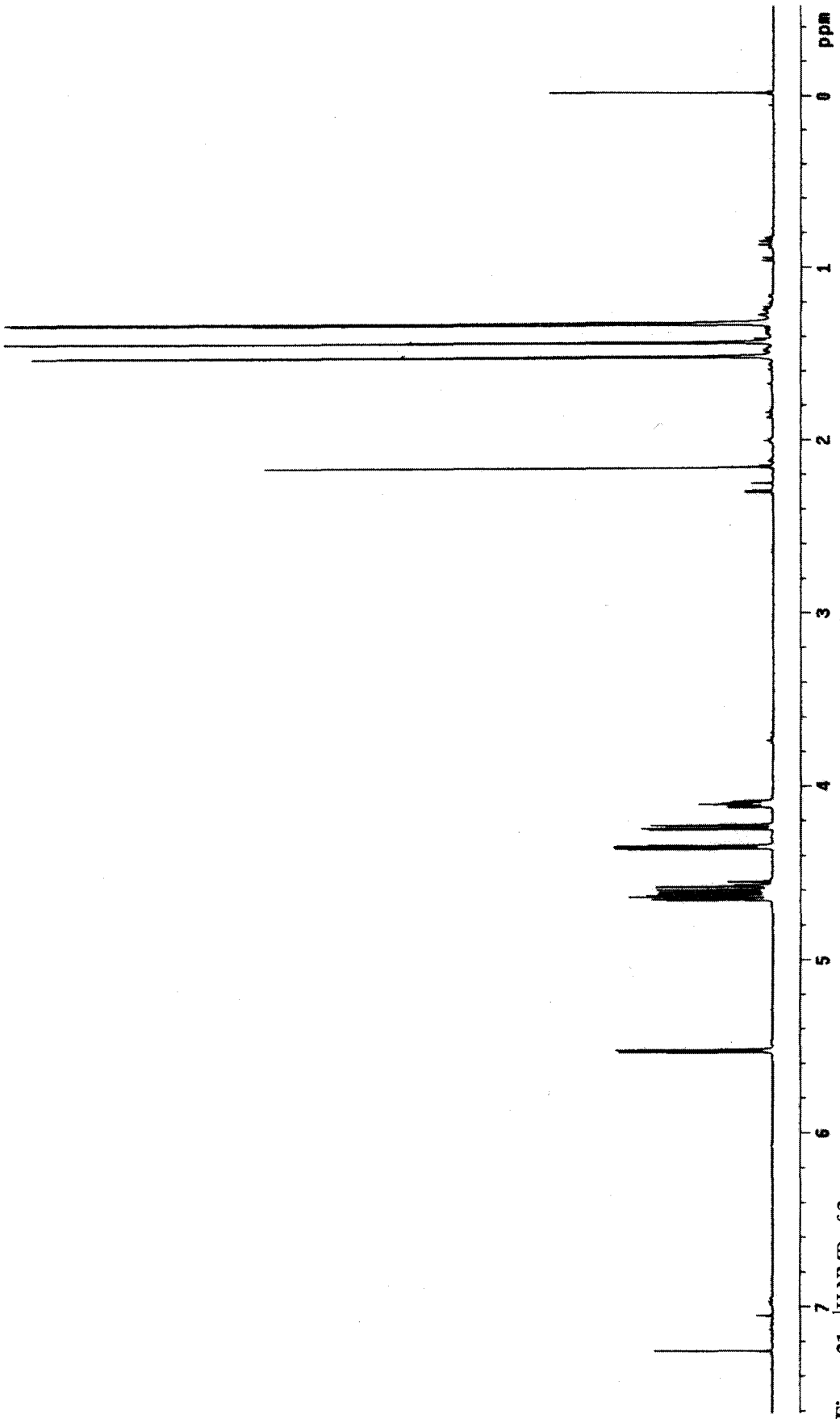

Figure 21. ^{1}H NMR of **3**

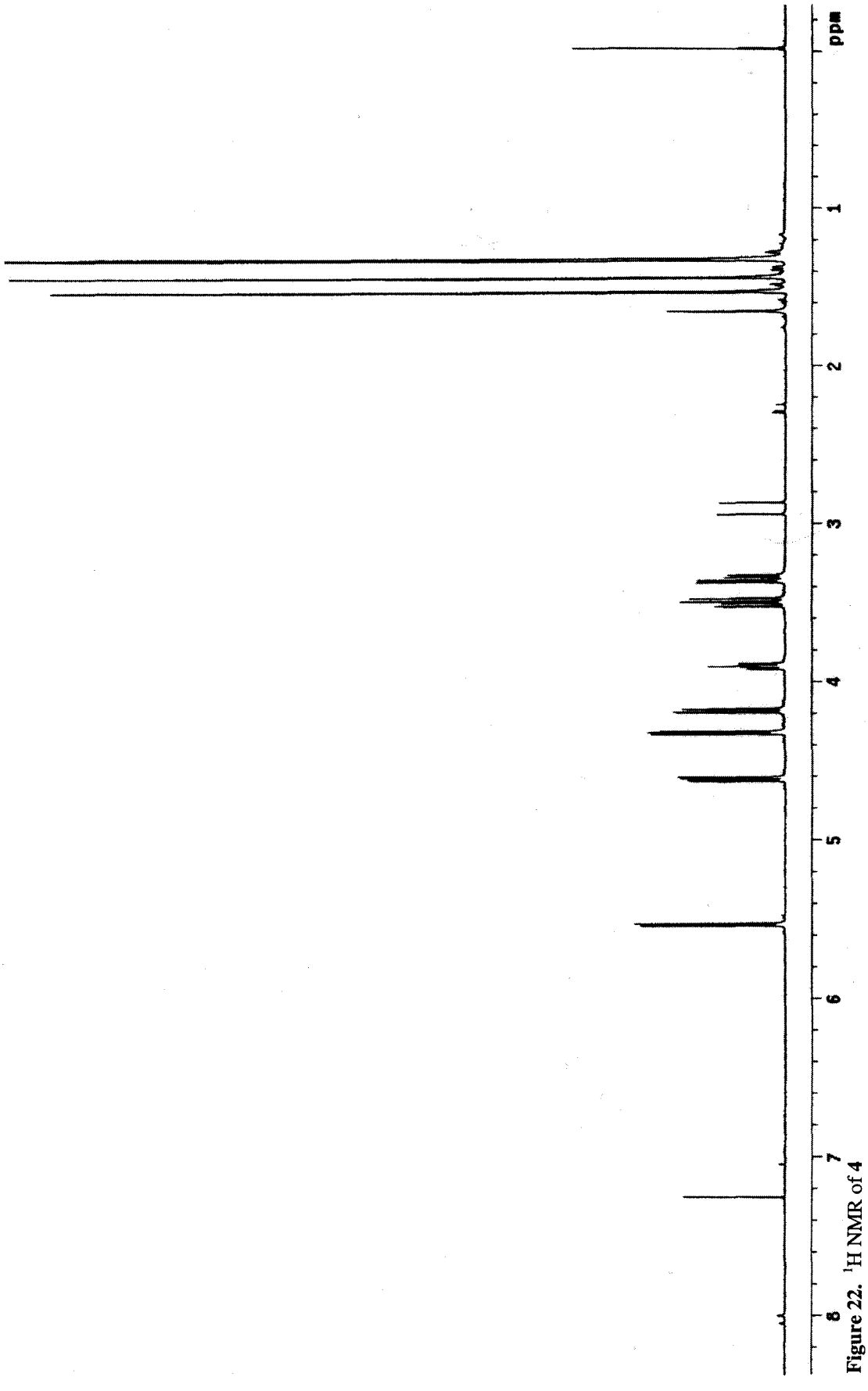

Figure 22. ^{1}H NMR of **4**

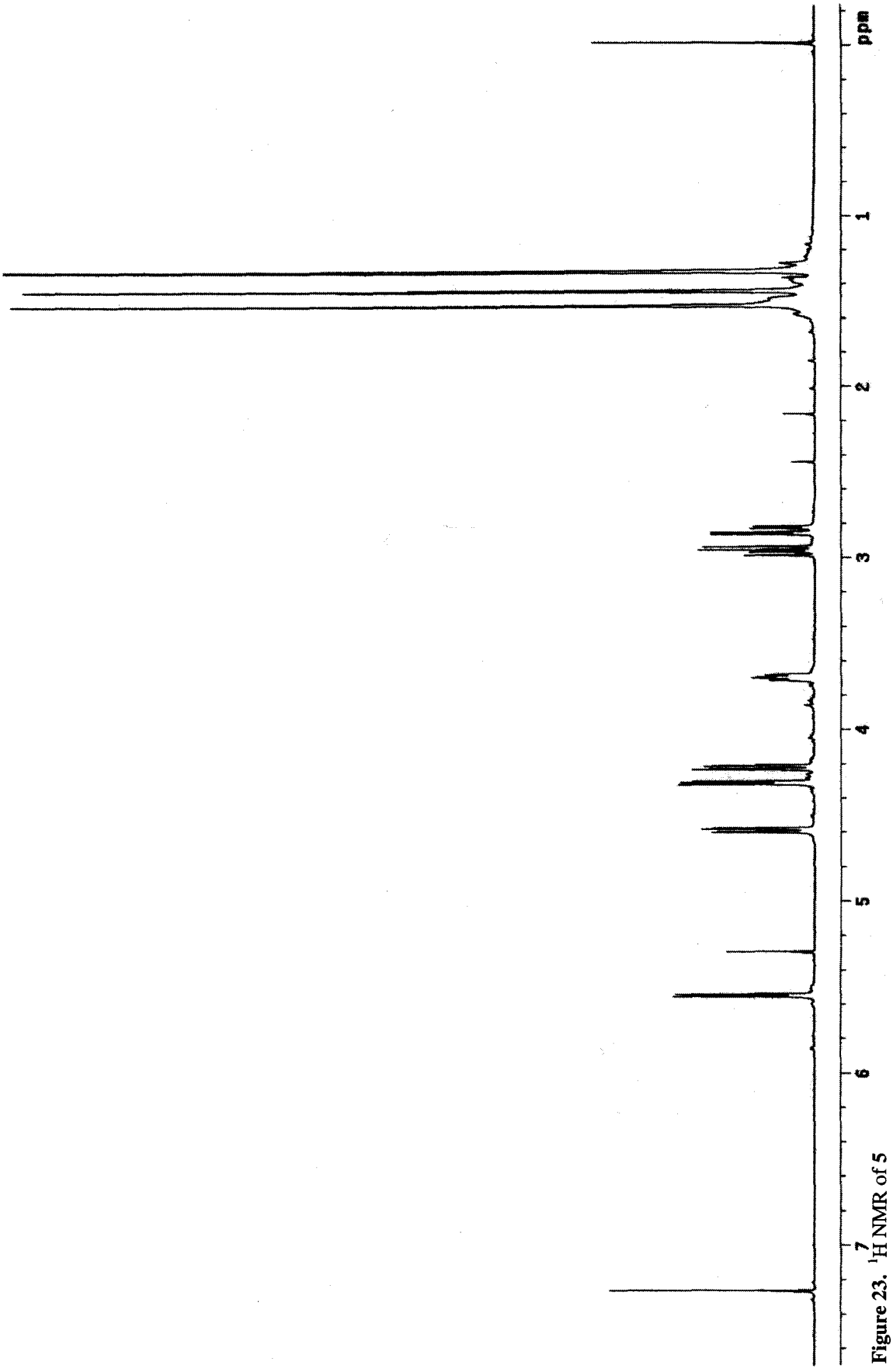

Figure 23. ^{1}H NMR of **5**

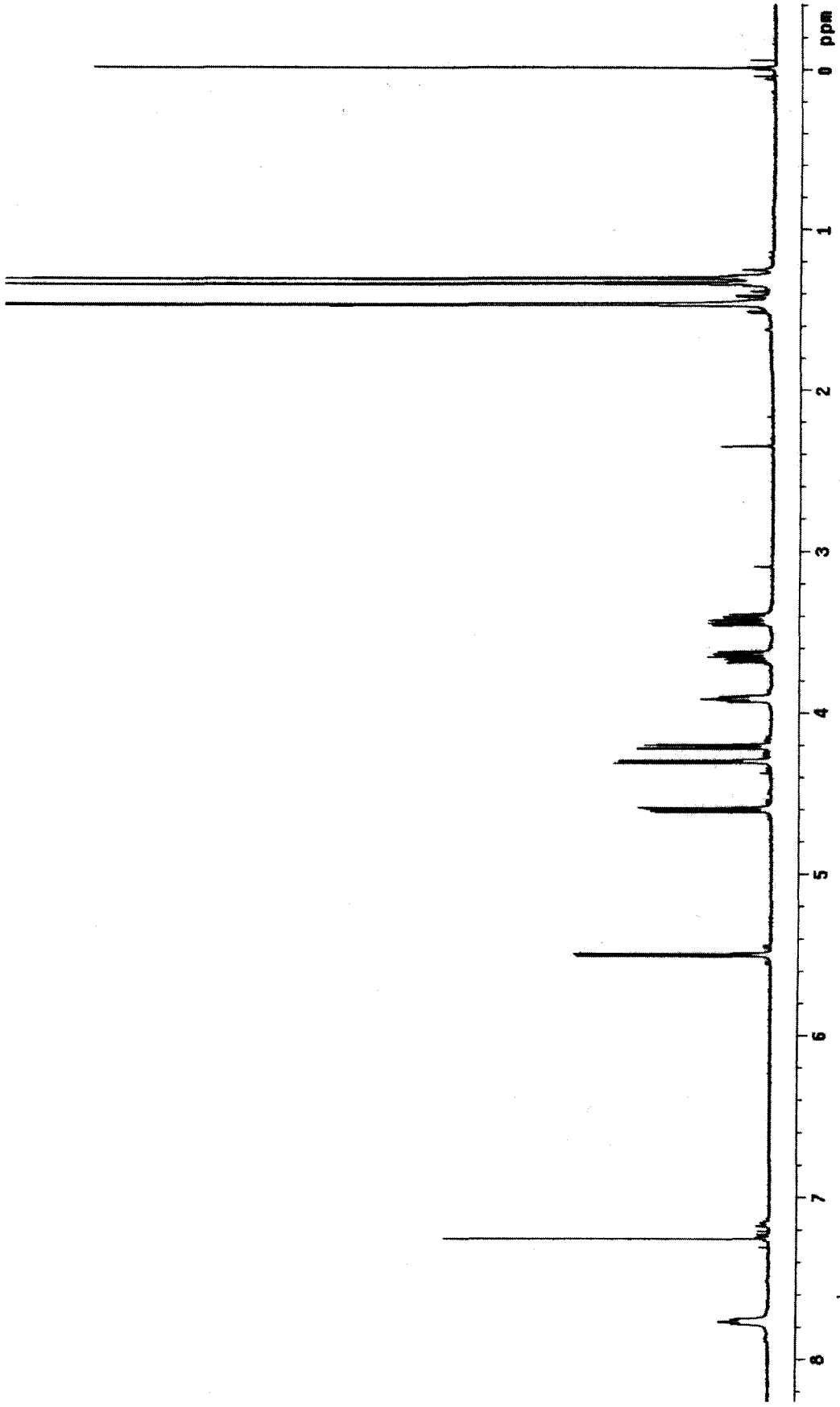

Figure 24. ^{1}H NMR of **6**

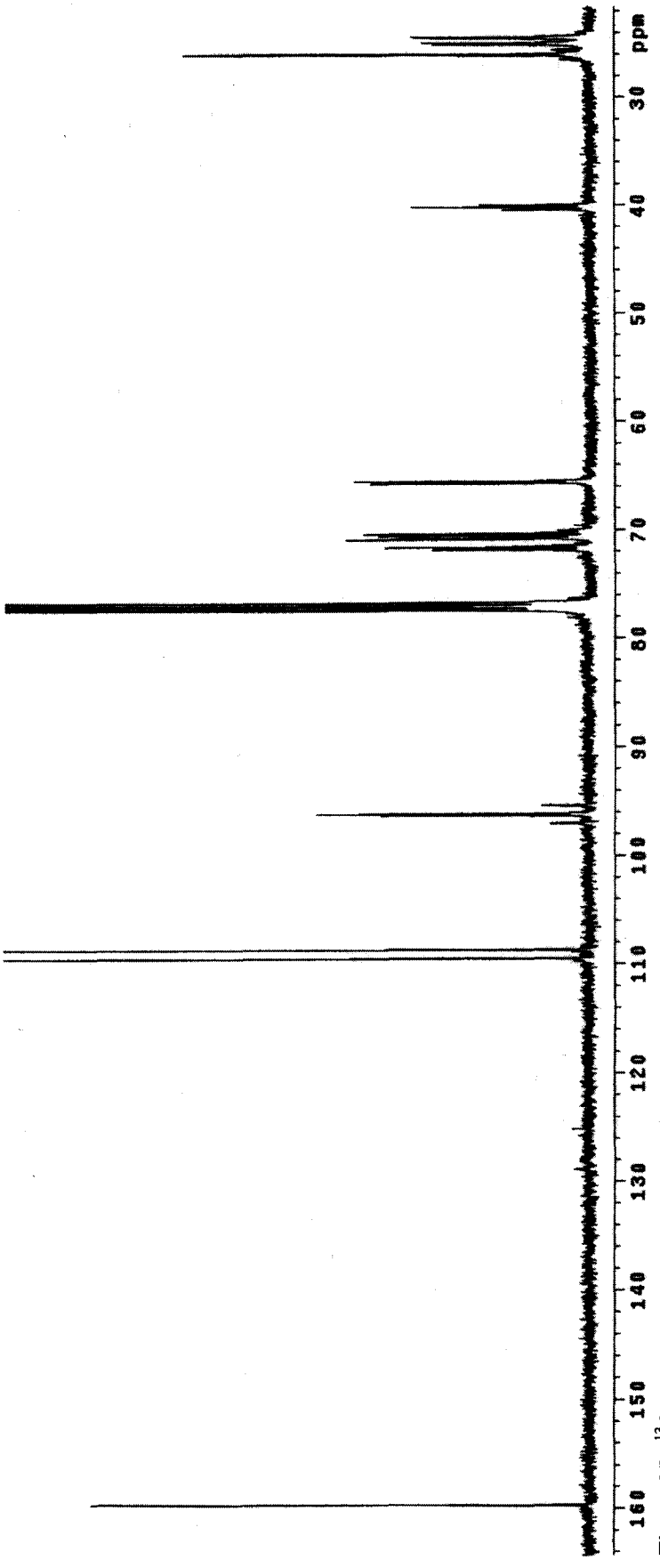

Figure 25. ^{13}C NMR of *6*

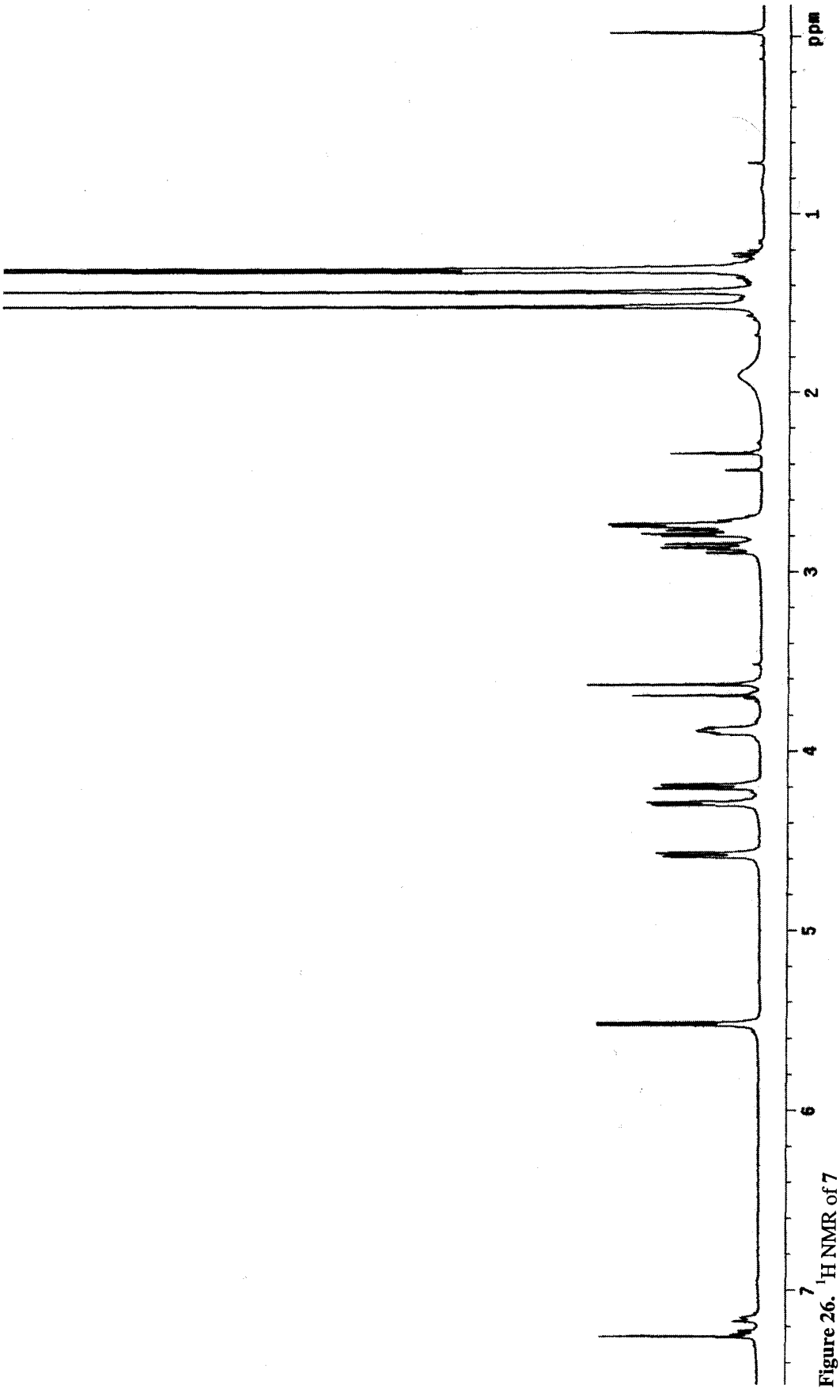

Figure 26. ^{1}H NMR of **7**

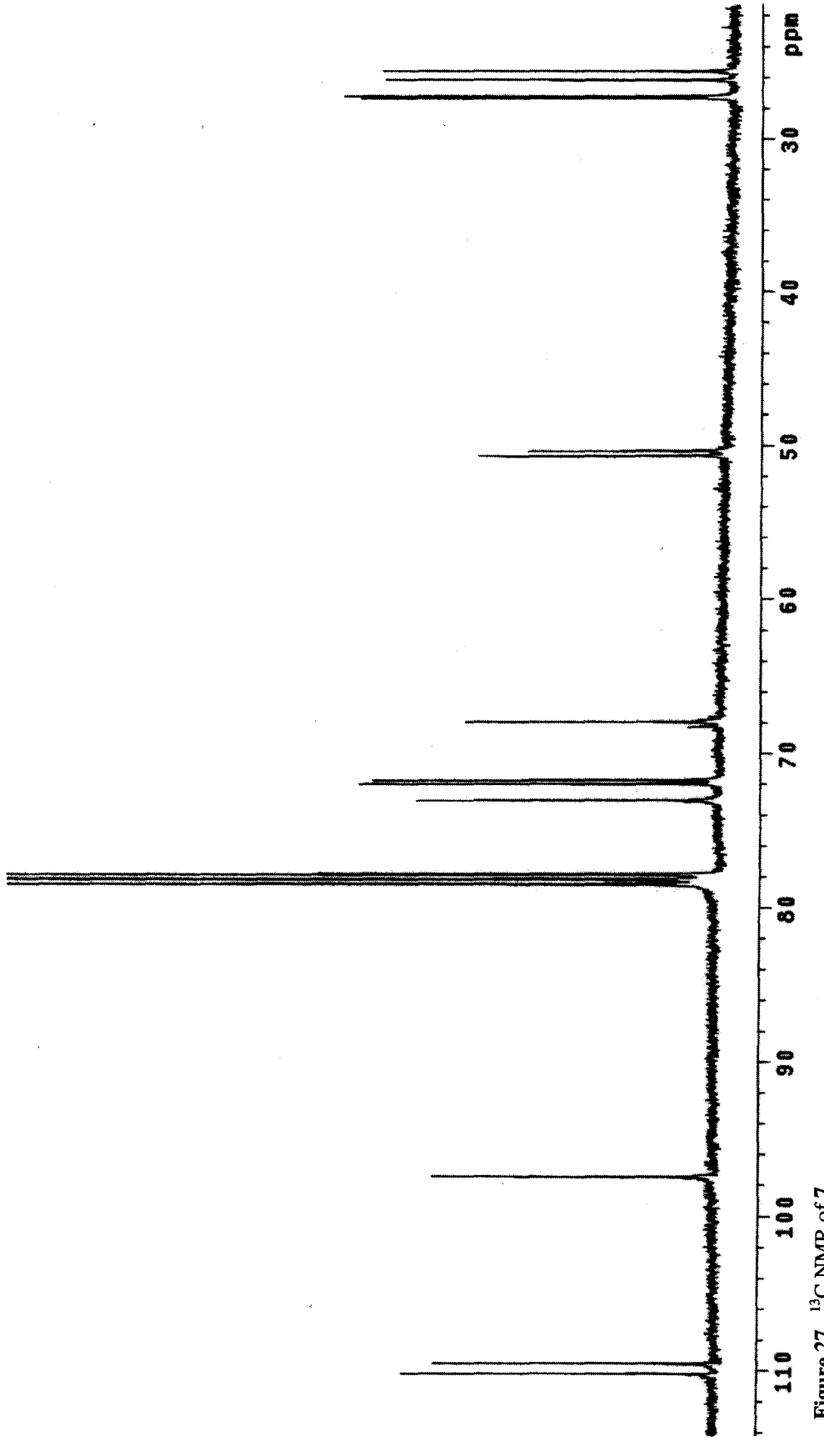

Figure 27. ^{13}C NMR of **7**

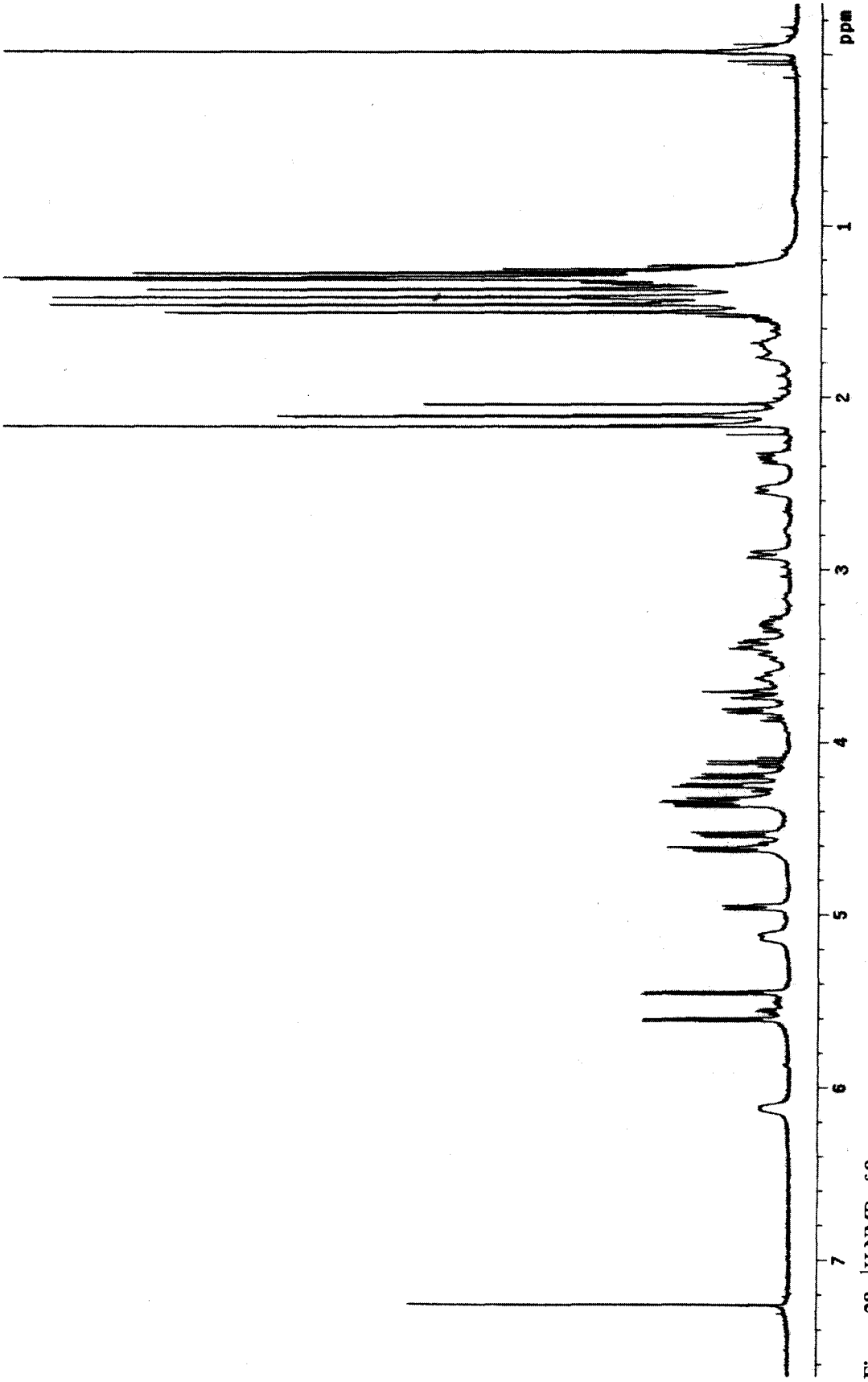

Figure 28. ^{1}H NMR of 8

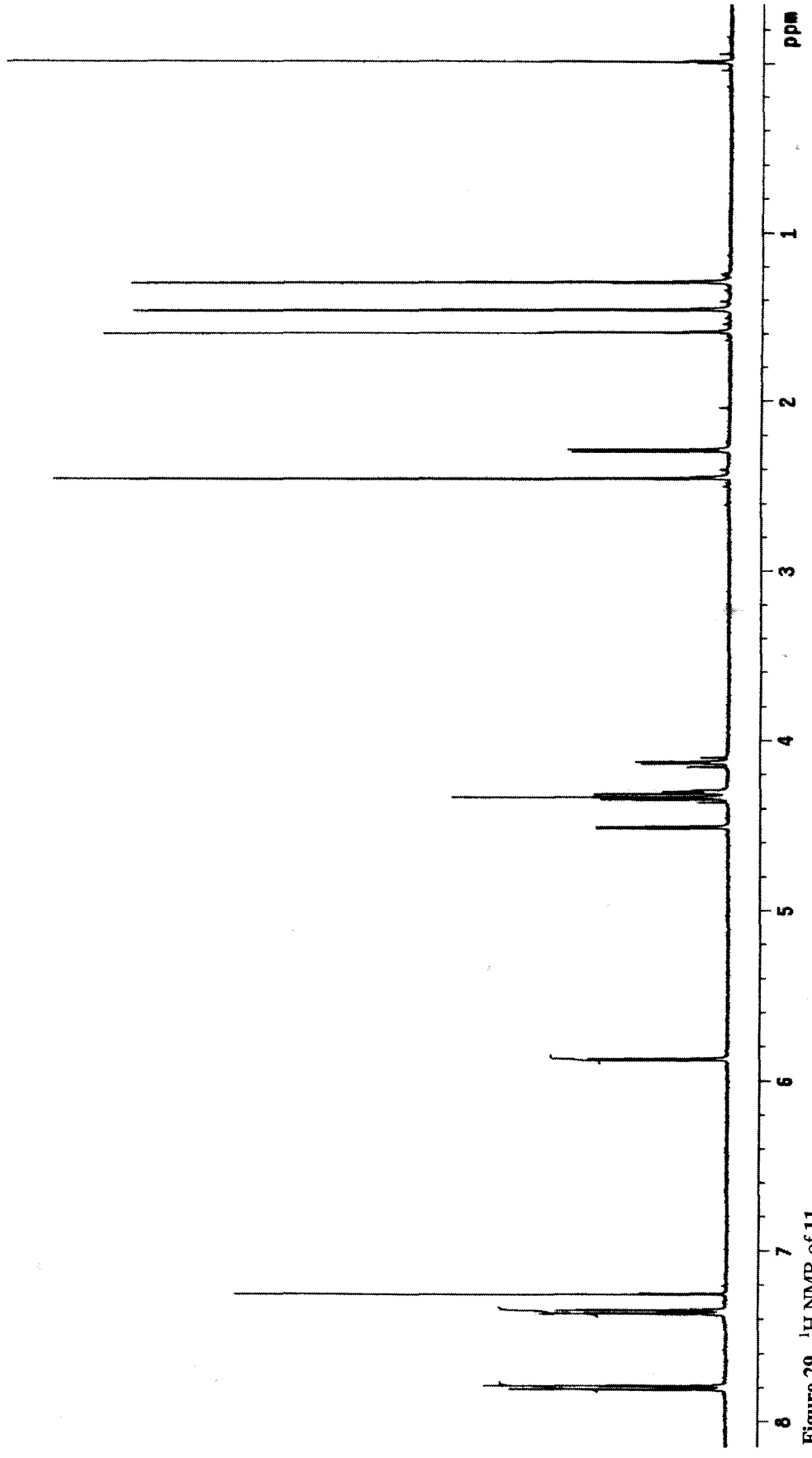

Figure 29. ^{1}H NMR of 11

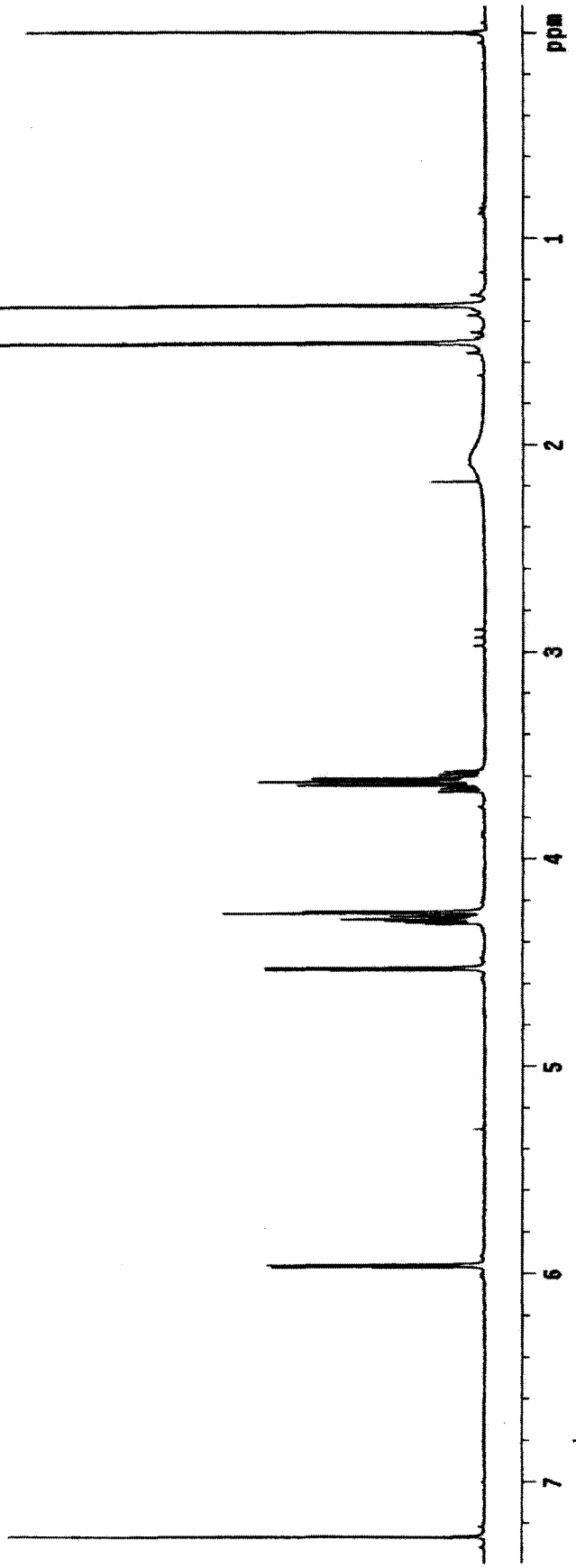

Figure 30. ^{1}H NMR of **12**

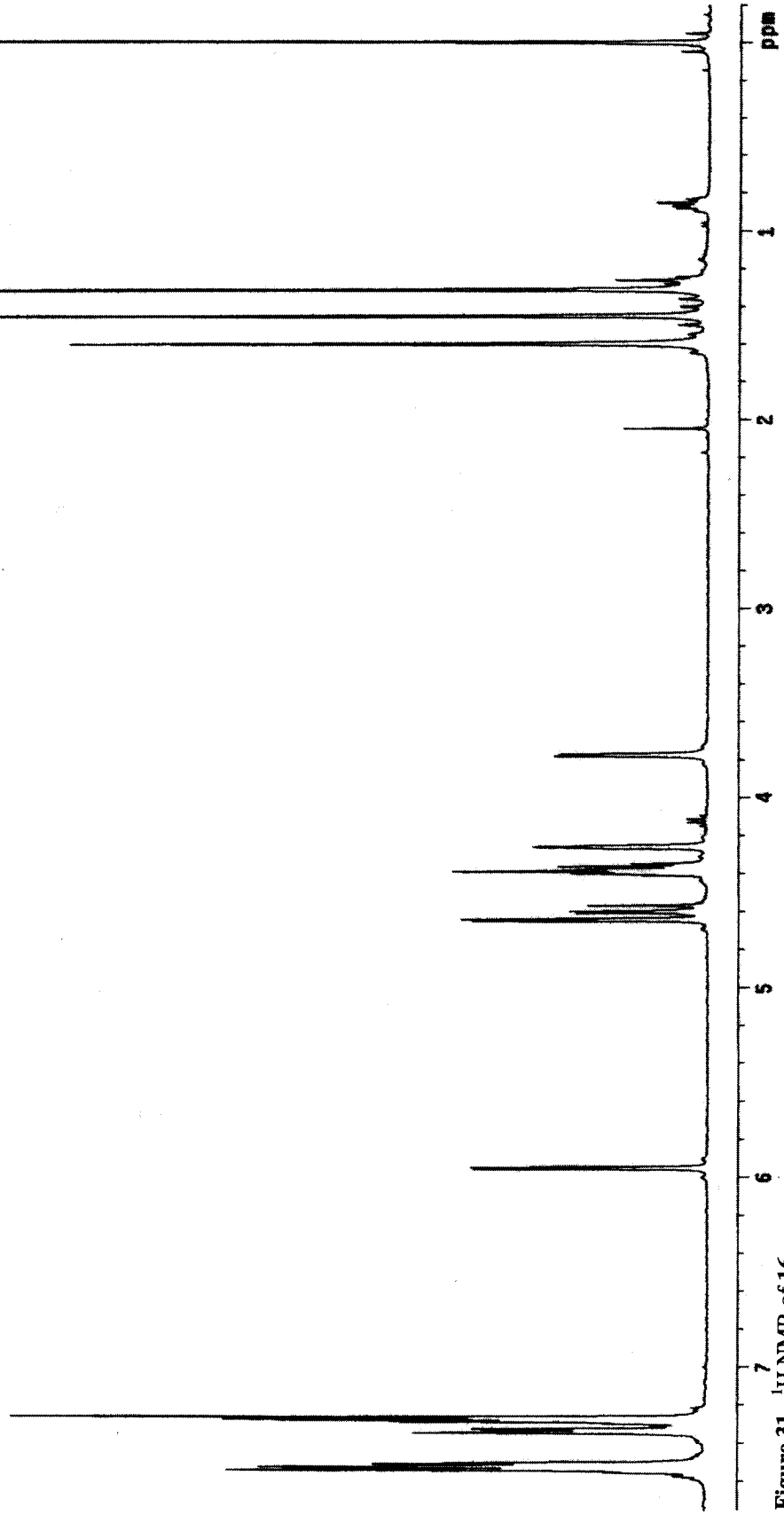

Figure 31. ^{1}H NMR of **16**

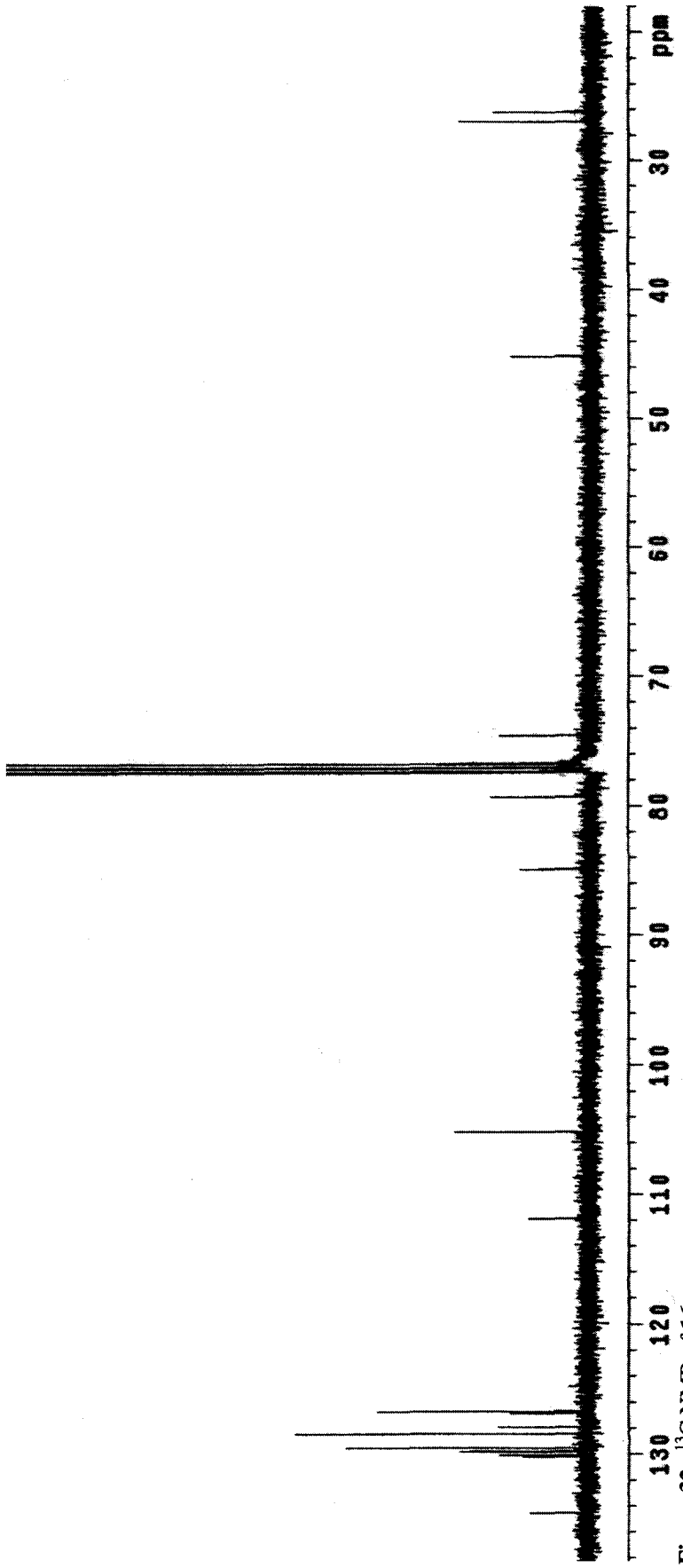

Figure 32. ^{13}C NMR of **16**

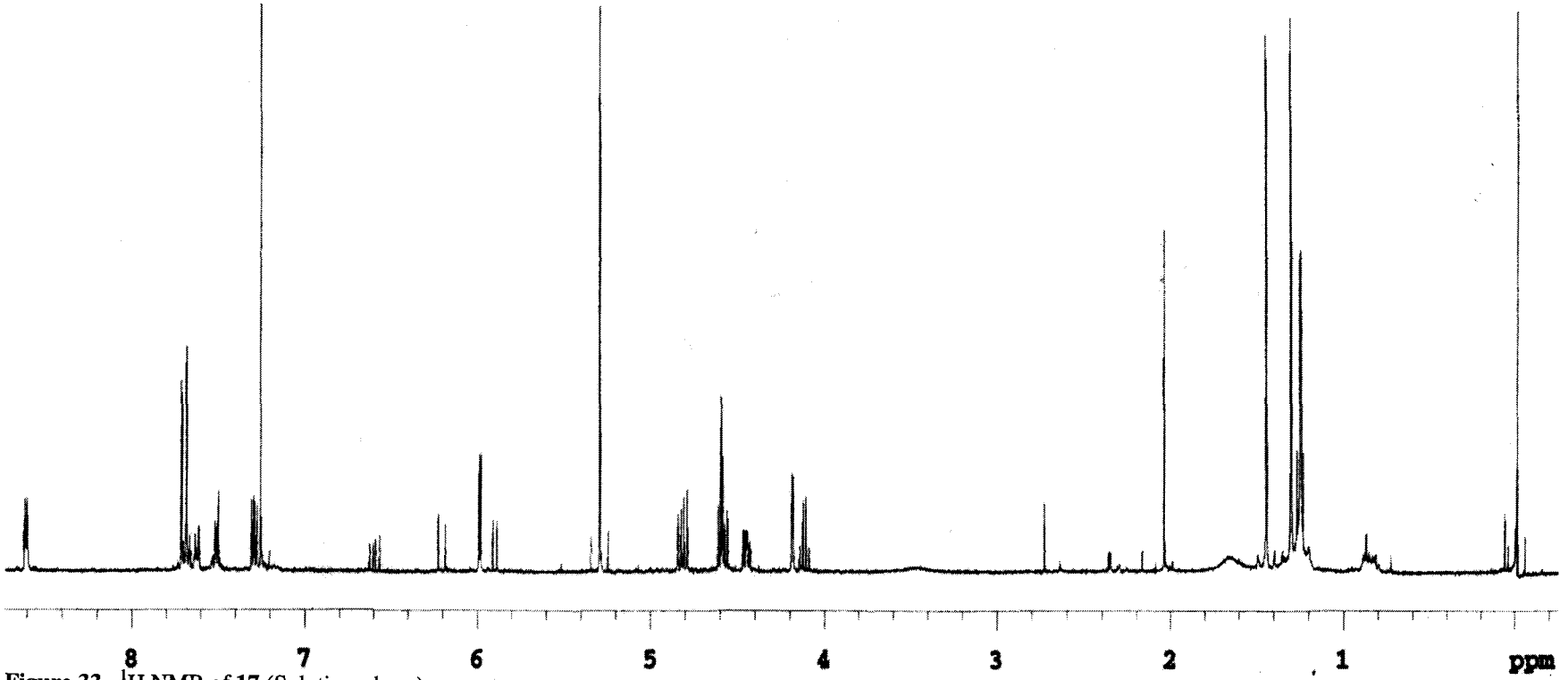

Figure 33. ^{1}H NMR of **17** (Solution-phase)

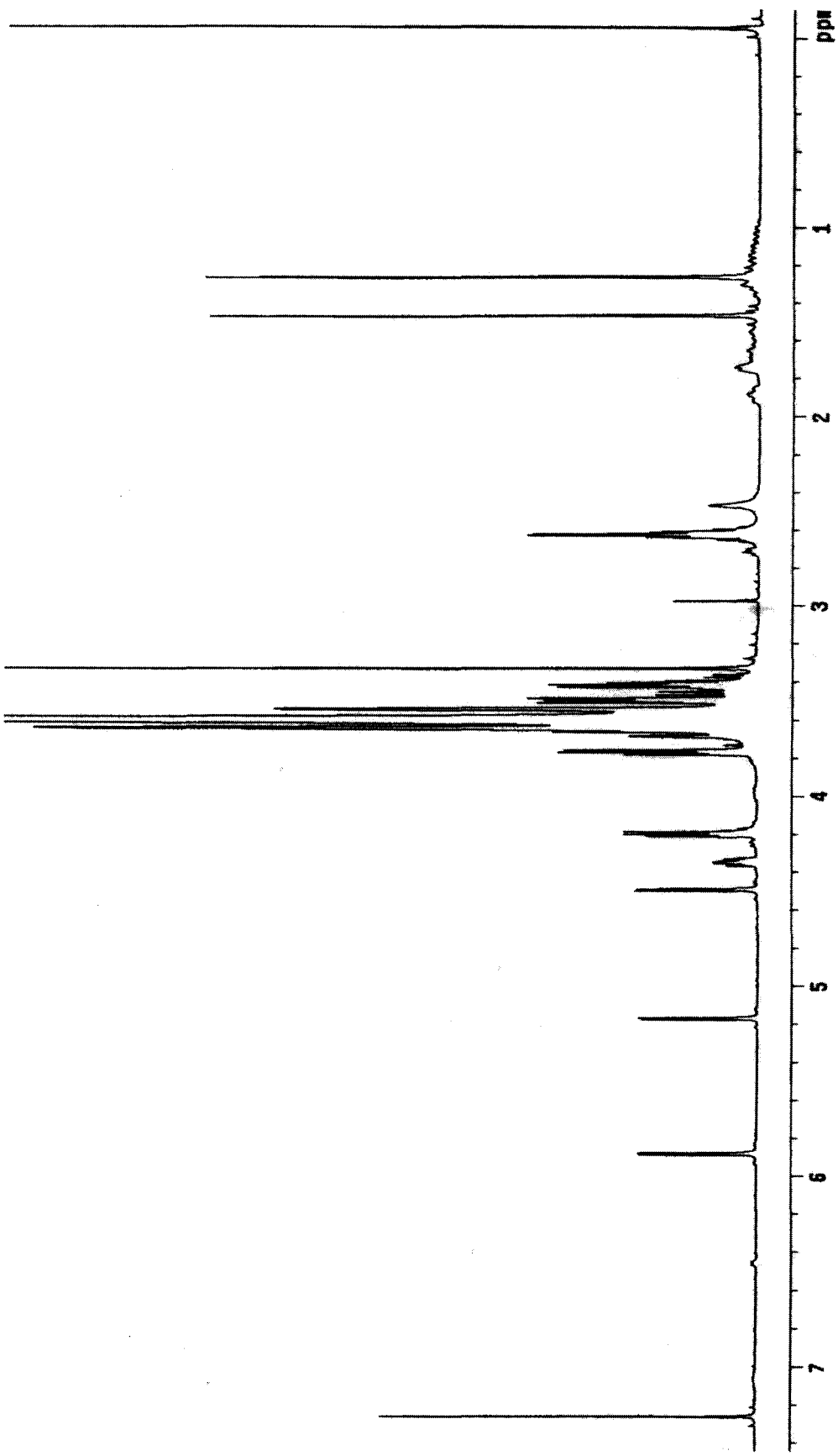

Figure 34. ^{1}H NMR of **20**

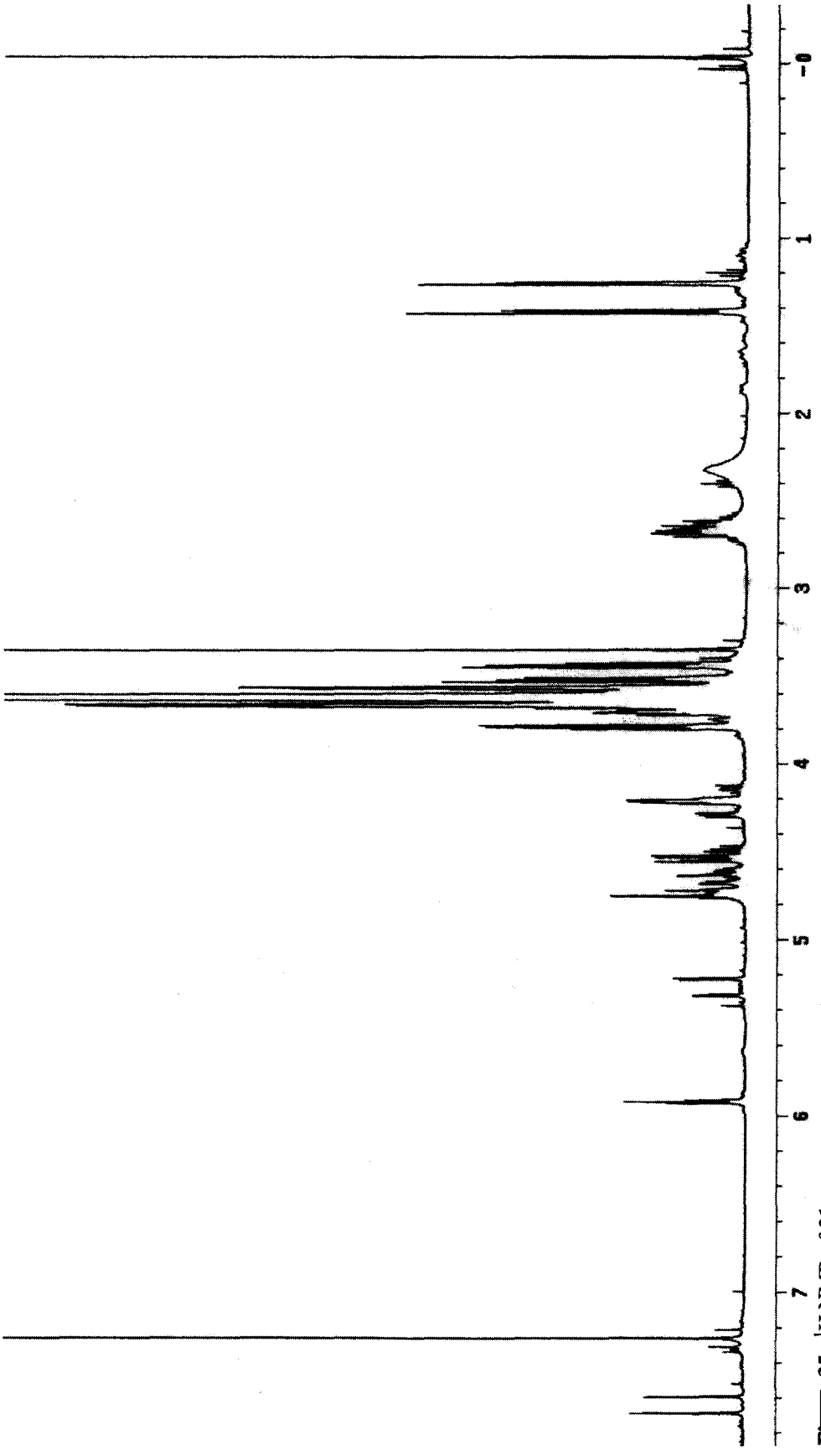

Figure 35. ^{1}H NMR of **21**

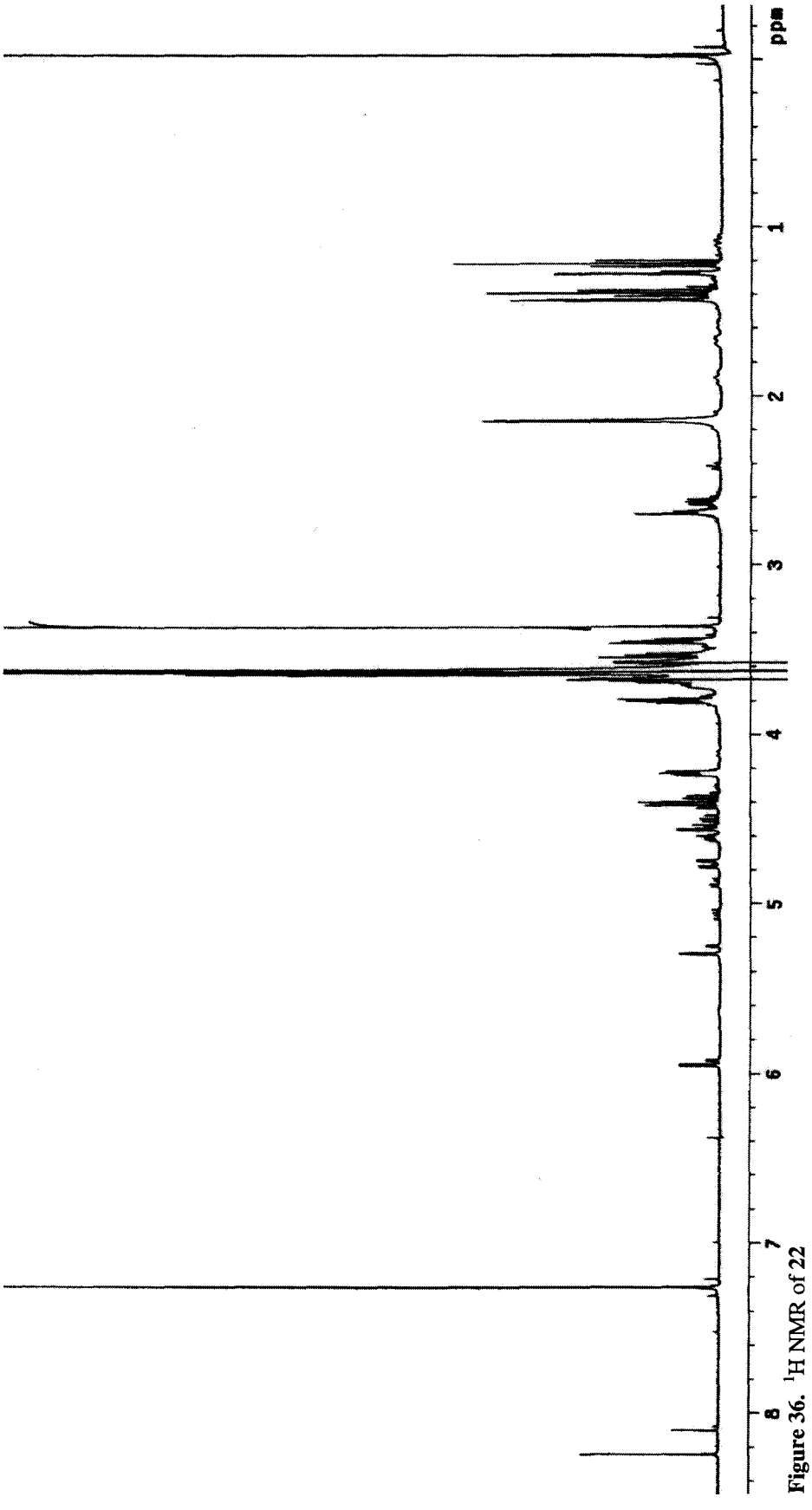

Figure 36. ^{1}H NMR of **22**

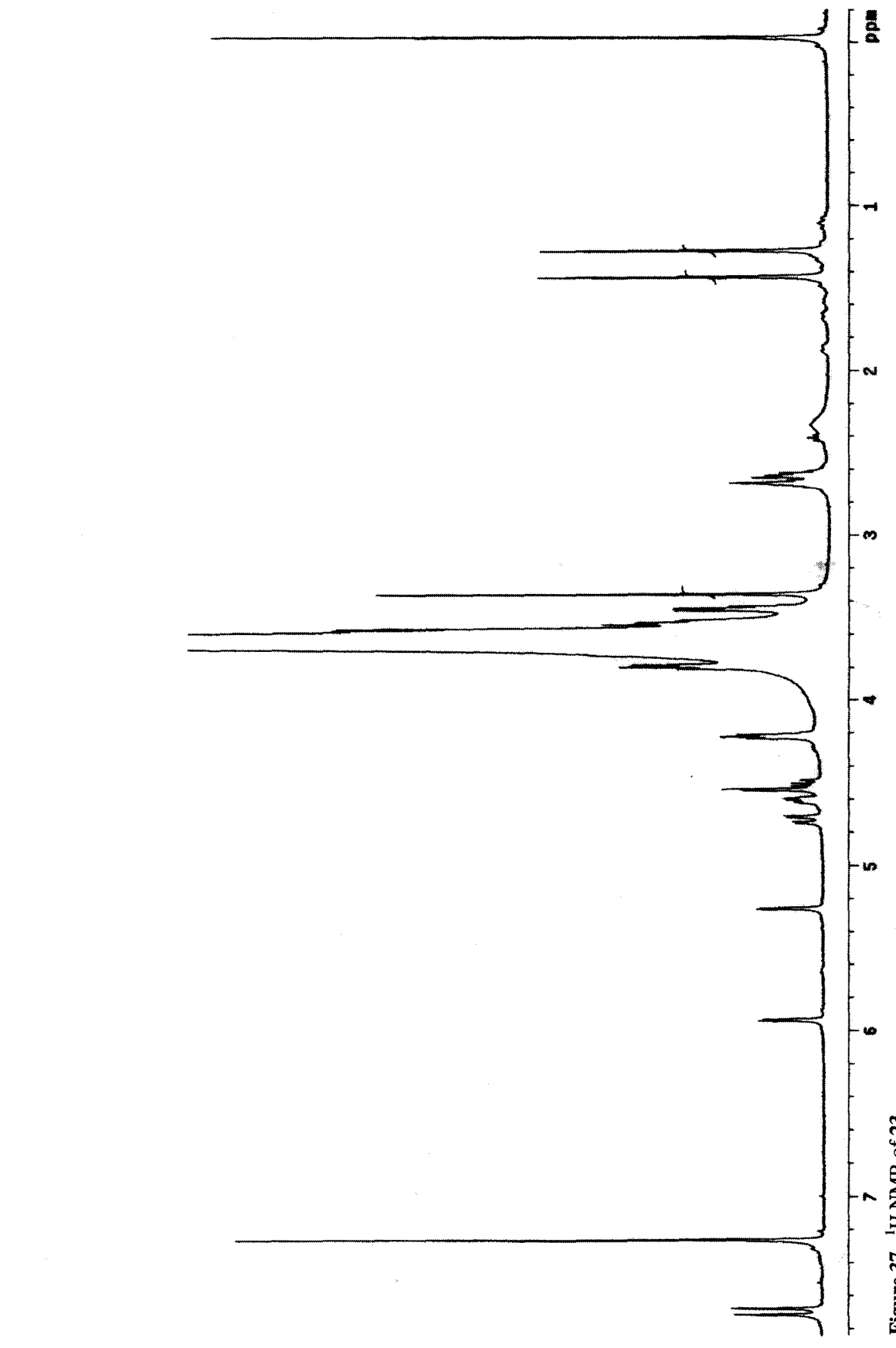

Figure 37. ^{1}H NMR of **23**

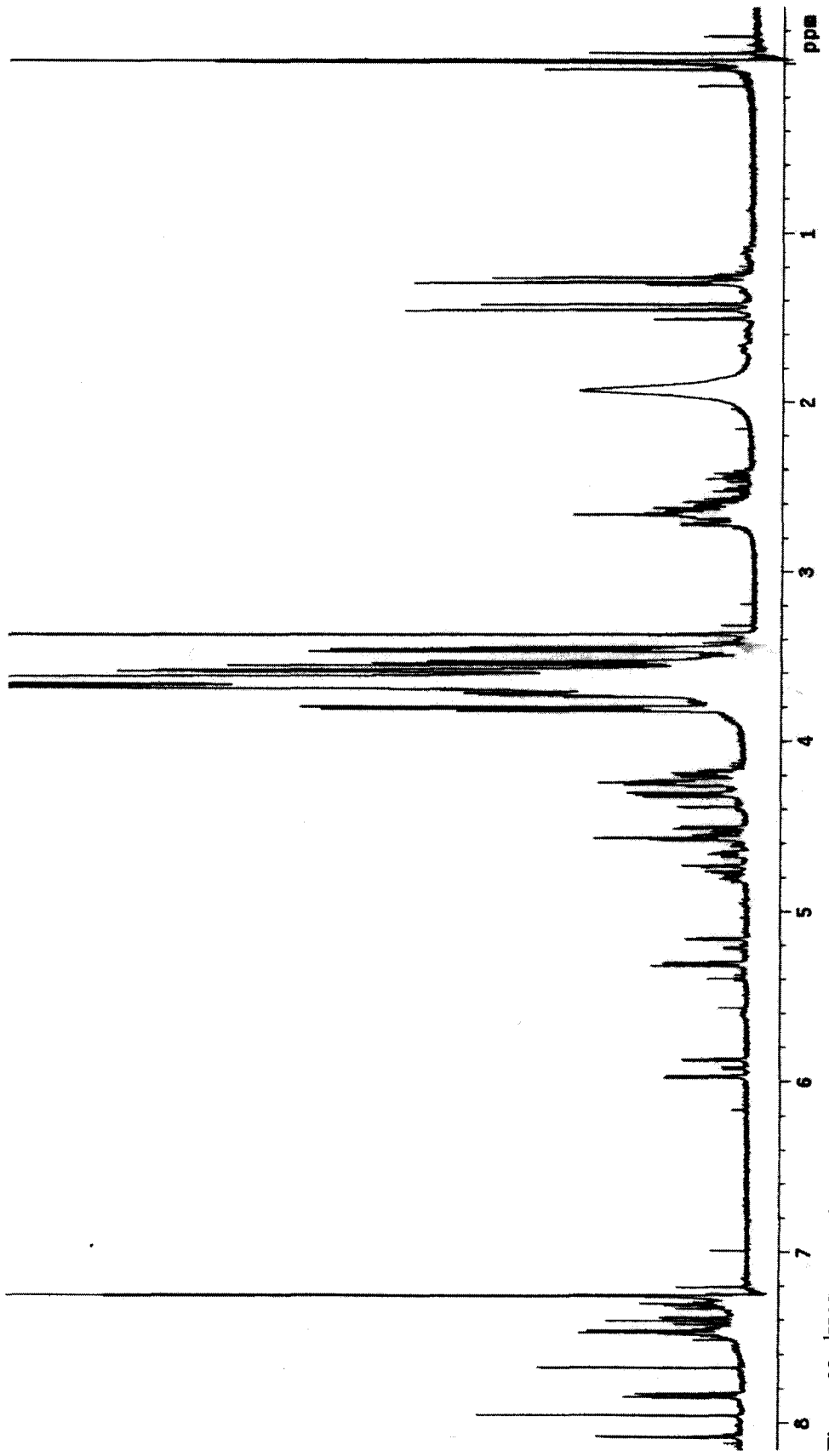

Figure 38. ^{1}H NMR of 24

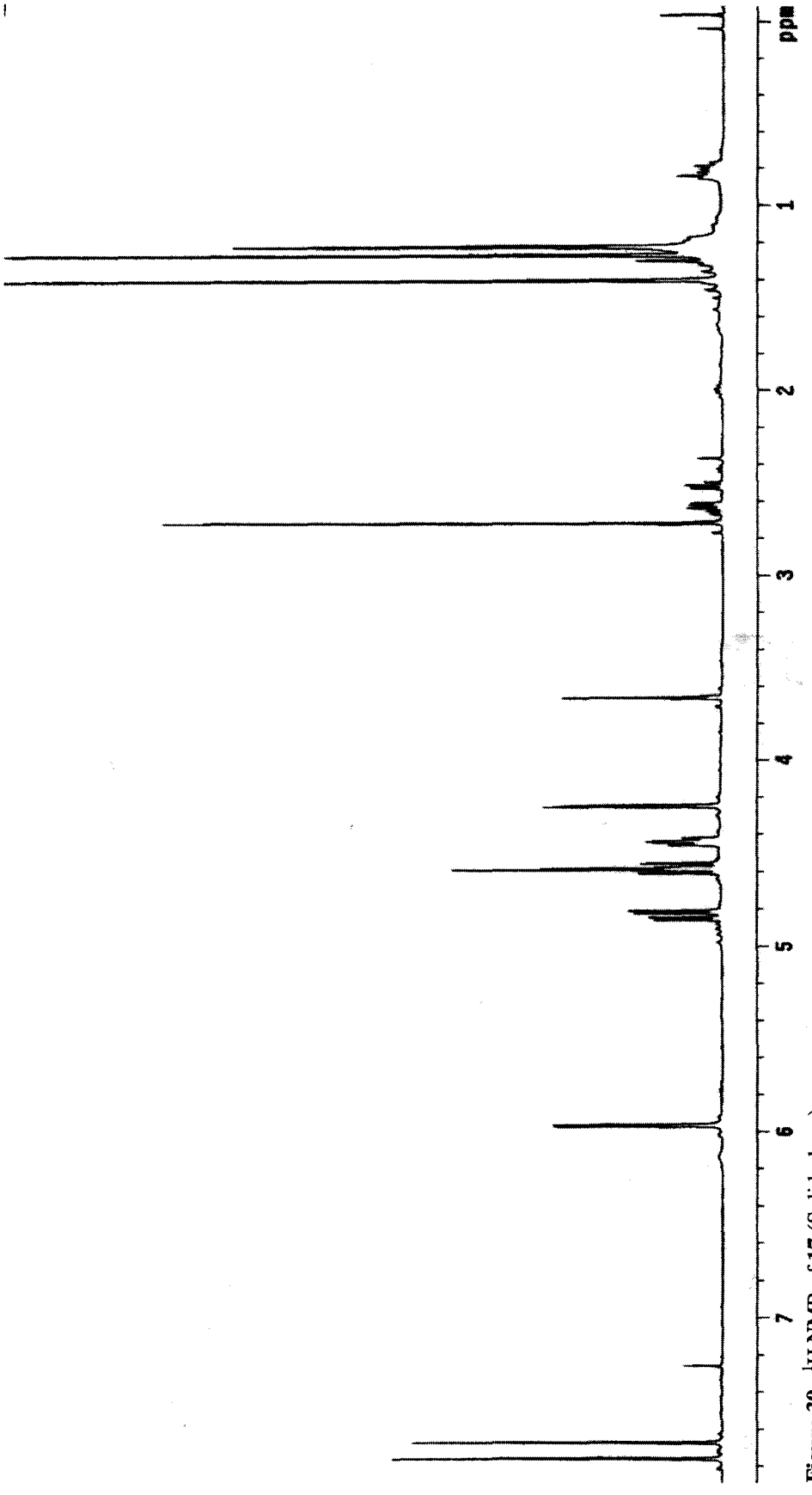

Figure 39. ^{1}H NMR of **17** (Solid-phase)